RESIN TRANSFER MOLDING (RTM) OF WOOD STRANDS REINFORCED COMPOSITE PANELS

By

WENRUI YANG

A thesis submitted in partial fulfillment of

the requirements for the degree of

Master of Science in Materials Science and Engineering

WASHINGTON STATE UNIVERSITY

School of Mechanical and Materials Engineering

August 2014

To the Faculty of Washington State University:

The members of the Committee appointed to examine the thesis of WENRUI YANG find it satisfactory and recommend that it be accepted.

Vikram Yadama, Ph.D. (chair)

Karl R. Englund, Ph.D.

Lloyd V. Smith, Ph.D.

Acknowledgement

I first need to express my appreciation to my advisor Professor Vikram Yadama. Throughout this endeavor, he has been enthusiastic, positive and pro-active towards helping me reach this goal. Were it not for our mutual desire to advance the field of high performance wood composites and his belief in my abilities, I likely may not have had this opportunity. I still remember those conversations when he talked to me as a friend and gave me courage and made me believe all the possibilities not only in research but also in life. Because of him, I learned how what is erudite and humble. I would also like to express my gratitude for the encouragement given from several of my professors including Professors Lloyd Smith, Karl Englund. These men conduct themselves with high ethics, integrity, and good senses of humor. They have quite active thoughts toward this area. It has been an honor to have them in my committee.

I especially need to extend thanks to Bob Duncan, Scott Lewis, They take great pride in their work and have always been an excellent resource for practical engineering problems. I also want to acknowledge Wanda Terry, Suzanne Hamada and Mary Simonsen for their excellent work in assisting grad students. I also appreciate Miles Pepper and Gary Held for making the acrylic mold for us. Thank you CMEC for providing great work place for research.

I would also extend my special thanks to my research partner, Guillaume, Denis Polskiy, Jonathon Waldrip. Those days I shall never forget: working together, solving all the problems, and enjoying exciting moments. Without their help, support and trust, I will never make this happen. Also of significant help during the two years study and research are my fellow grad students and friends: Arun Garg, Wenjia Song, Raul, Rui Zhu, Yu Wang, Fang Chen, Chao Zhang. Thank you for the technical discussion and fantastic ideas.

The author is appreciated to CCP Composite, Ashland, AOC for providing the resins; ChemTrend for providing release agent.

This study is based upon work partially supported by the National Science Foundation under Grant No.1150316.

My highest expression of thanks goes to my parents and sisters. They have been a continual source of love, encouragement and support while I pursued this goal. My parents encouraged constantly and unconditionally. I shall share this happiness with you. My sister Wenjun Yang, she put her endeavor in my research and gave me suggestions which made me look forward and gain me strength. I could not have done this without them.

RESIN TRANSFER MOLDING (RTM) OF WOOD STRANDS

REINFORCED COMPOSITE PANELS

Abstract

by Wenrui Yang, M.S.
Washington State University
August 2014

Chair: Vikram Yadama

Resin transfer molding (RTM) and vacuum assisted resin transfer molding (VARTM) are widely applied in manufacturing airplane and automobile interior composite products due to their cost-effectiveness. In implementing this manufacturing technology, resin impregnation is critical to the quality of composite products. Since permeability of wood strands preform (the fiber reinforcement) affects the resin impregnation, resin flow and permeability behavior should be understood to produce quality products with consistent performance. This study focused on determining suitable processing variables for preform fabrication and characterizing resin flow and physical and mechanical performance of composite panels.

Cold setting adhesive (PVAc) applied to discontinuous elements, wood strands, solely for the purpose of pre-pressing a preform to maintain its form and integrity. Design of experiments (DOE) was utilized to statistically analyze the influence of processing variables, PVAc content and preform target density. A linear model was developed using response surface method (RSM) for the determination of ideal processing parameters in resin transfer.

Preform permeability was calculated based on Darcy's law using three different approaches. Results indicated increasing trends in permeability estimation with increased injection pressure and decreased vacuum. Surface finish showed a direct relationship with increased vacuum. Composite panel flexural behavior was directly proportional to preform density.

Benchmark property values for RTM manufactured wood strand composite panels were established, that has not been done before. Panels exhibited excellent mechanical properties and moisture resistance (an indirect measure of dimensional stability); among the three resins evaluated, vinyl ester yielded better flexural, tensile, internal bond, moisture sorption properties.

Table of Contents

List of Table

List of Figures

Chapter 1 Introduction and Literature Review

1.1 Introduction

Fiber reinforced polymer (FRP) composites are widely applied in automobile, aviation, and defense-related industries due to their excellent performance in specific strengths compared to traditional materials such as metals or pure polymers (Deacon, 2012). Natural fibers are gaining importance as reinforcing fibers with demand for renewable materials. Engineering wood composites, along with other natural fiber composites, can be tailored for different applications. They provide an advantage of utilizing small diameter timber and faster growing plantation trees, generally of lower quality, to produce higher performance products for value-added applications.

Resin transfer molding (RTM) or vacuum assisted resin transfer molding (VARTM) is a closed molding technique that can produce medium volume panels with desired dimensions and finished surfaces. Due to the cost-effectiveness, RTM has been applied successfully in airplane interior decor and the automobile industries (Verrey, Wakeman, Michaud, & Månson, 2006). RTM can be adopted in wood composite industries but a good understanding of the influence of processing variables for producing high performance composite products using discontinuous wood elements is essential.

1.2 Objective

The overall project goal is to contribute to an understanding and developing of the underpinning science and technology of resin transfer molding (RTM) wood strands composite products for a wide array of applications, including automobile, aerospace, and building industry. The primary objective of this research is to conduct preliminary analysis of the relationships between RTM processing factors and the performance of wood strands composite panels. This study will establish as to which factors are

significant and indicate the general trend of their influence. Three sub-objectives were undertaken to meet the primary goal:

1) Study the influence of wood strands preform parameters on the RTM process for suitable preform fabrication.
2) Identify the influence of preform and resin characteristics on physical and mechanical properties of molded composite panels.
3) Establish benchmark performance values for RTM produced wood strand composite panels.

1.3 Impetus

Many researchers have studied the synthetic fibers, especially carbon and aramid or Kevlar fibers, as reinforcement in polymer resin matrices (Barraza, Hamidib, Aktasb, O'Rear, & Altan, 2004; Deacon, 2012; Holmberg & Berglund, 1997; Lee, Lee, Jang, Lee, & Nam, 2002). Limited research has been done on manufacturing natural fiber reinforced composites using the RTM process (Table 1.1). Given that RTM is widely used to produce geometrically complex and cost-effective composite products, authors found no research conducted on wood strands reinforced composite products using RTM technology. RTM has advantages over other closed molding technologies like compression molding and vacuum infusion (Lacovara, 1995). These advantages include low tooling cost, room temperature processing and less styrene emission.

Narrow wood flakes produced by shaving logs lengthwise using knives are referred to as wood strands. Unlike a particle, a fiber, or a wafer, a wood strand has a large enough aspect ratio enabling transfer of shear forces from matrix to fibers, thus utilizing the strength capacity of the fiber resulting in stronger composite. A wood strands as an oriented natural fiber has many mechanical and cosmetic advantages. It has been widely used in making oriented strand board (OSB), and is widely used in residential and commercial construction and furniture production. Nevertheless, the limitation of relatively stable demand from housing and furniture urges traditional forest products to expand into new markets.

Therefore, the focus of this study is to understand the influence of preform structure and processing factors in producing wood strand composite panels using RTM technology, potentially for higher value product applications in automobile and/or aerospace industries.

Table 1.1 Materials been used in RTM

Fiber	Resin
Glass fiber	Unsaturated polyester resin/PVAc and PMMA (Haider et al., 2007)
Jute fiber	PVC (Khan et al., 2011)
Sisal fiber	Vinyl ester (Li, 2006)
Kevlar fabric/carbon fiber	Epoxy (Deacon, 2012)
Hemp fiber/ kenaf fiber	Unsaturated polyester (Rouison et al., 2004)
Glass fiber	Epoxy (Barraza et al., 2004)
Woven jute fiber	Water/glycerin solution (Francucci & Vázquez, 2012)

1.4 Literature Review

A brief review about natural fibers used as reinforcement in RTM composite products is provided in this section. Review will emphasize the prediction of permeability and the impact of important processing variables.

1.4.1 Permeability

Resin impregnation is determined by injection pressure, vacuum, preform architecture, preform permeability, and resin property. Therefore these processing variables were taken into consideration in the study. Permeability indicates the relative ease at which liquid travels through porous medium. Permeability measurement has always been a difficult and controversial issue for different researchers (Ferland & Trochu, 1996). Studies have been conducted with an ASTM standard for permeability measurement (Conshohocken, 2014; Materials, Technique, & Ovens, 2014); however, those methods are

difficult to conduct and ambiguous for a wood strands preform. Due to the lack of a standard, many researchers have developed their own methods to measure the permeability.

Darcy's law (Siau, 1995)is probably the most commonly used in permeability prediction models. Preform permeability varies in three dimensions. Gebart and Lidström (1996) studied the in-plane permeability both in parallel flow and radial flow. They also distinguished the global coordinate from the principle coordinate systems, as well as the permeability at saturated fiber from the moving flow front. Parnas and Salem (1993) developed inter tow flow and intra-tow flow, which can be called macro-infiltration and micro-infiltration (Figure 1.1), respectively. This introduces differences in driving force for resin (Parnas & Salem, 1993). Therefore, the results for the two different resin flow mechanisms are different. In both cases the measurement of the permeability can be conducted with constant injection rate or constant injection pressure as initial and boundary conditions. Most researchers choose constant injection pressure because it is easier to establish. However, one drawback is that the initial resin velocity can be very high (Hoes et al., 2002).

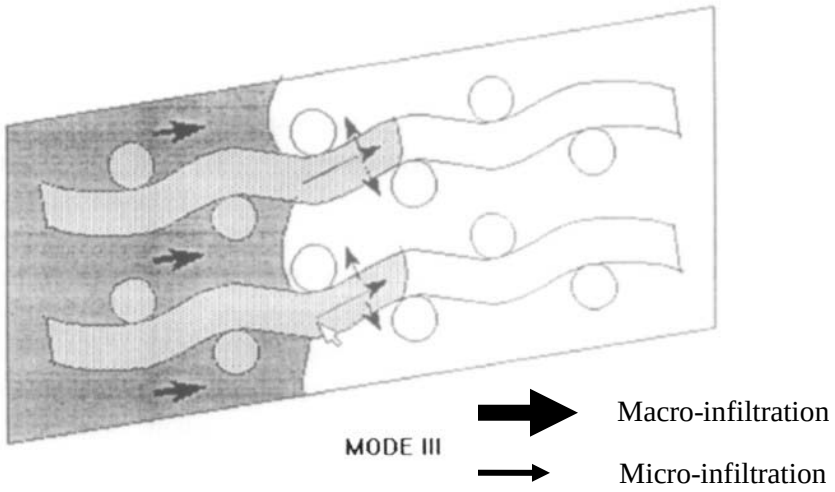

Figure 1.1 Macro-infiltration and micro-infiltration (Lekakou & Bader, 1998a)

Through thickness permeability is usually negligible due to a relatively small mold thickness in RTM or VARTM because the diffusion effect is relatively small. However, for fabricating thicker parts through

thickness permeability needs to be considered as diffusion effect will influence the resin flow. Besides Darcy's law, Kozeny-Carman equation has also been developed to predict the permeability. A Kozeny constant is introduced based on the fiber preform architecture (Deacon, 2012). Preform architecture and resin impregnation influence the preform permeability, thereby greatly affect the quality of the composite product in RTM process.

1.4.2 Processing Parameters

1.4.2.1 Preform Architecture

Preform architecture such as unidirectional, bidirectional, woven, knitted, yarn mats and random mats. Generally, permeability is often related to fiber volume fraction or porosity. Fiber preform porosity is defined as the fraction of the total volume of the voids besides fiber, usually denoted as $\emptyset$. It is the opposite of fiber volume fraction, denoted as v_f. Porosity is of vital importance of permeability, thus it affects the composite quality. Dong (2006) compared the filling time for fiber porosity and high permeable medium (HPM) porosity with response surface method (RSM). However, limited experimental data makes it equivocal to choose a proper flow media. Fink et al. (2000) studied the influence of distribution medium porosity to flow front velocity and fill time (Figure 1.2). Increasing the porosity of the distribution medium will slow down the flow front and increase the fill time. A recent review by Naik et al.(2014) conclude that transient permeability is directly related to porosity (Figure 1.3). Other researchers studied the architecture of fiber preform, which mainly focused on the woven patterns and fiber volume fraction by varying the preform layers (Advani, Bickerton, Sozer, & Graham, 2000; Gokce, Chohra, Advani, & Walsh, 2005) or varying compression pressure (Buntain & Bickerton, 2003). Arbter et al. (2011) concluded permeability increases with decreased fiber volume fraction through literatures. Rouison et al. (2006) studied the tensile and flexural properties with different fiber volume fractions. Higher fiber content resulted in higher mechanical performance.

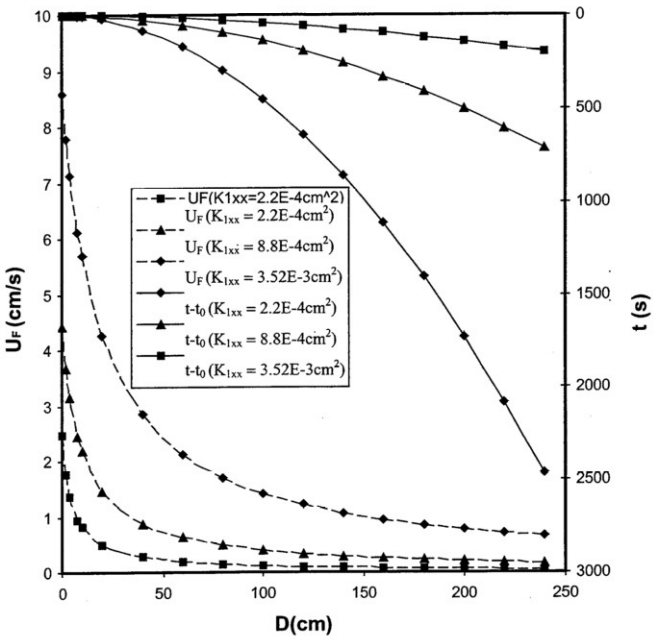

Figure 1.2 Flow front velocity and fill time as a function of length of the saturated region: effect of permeability of distribution medium (Fink et al., 2000).

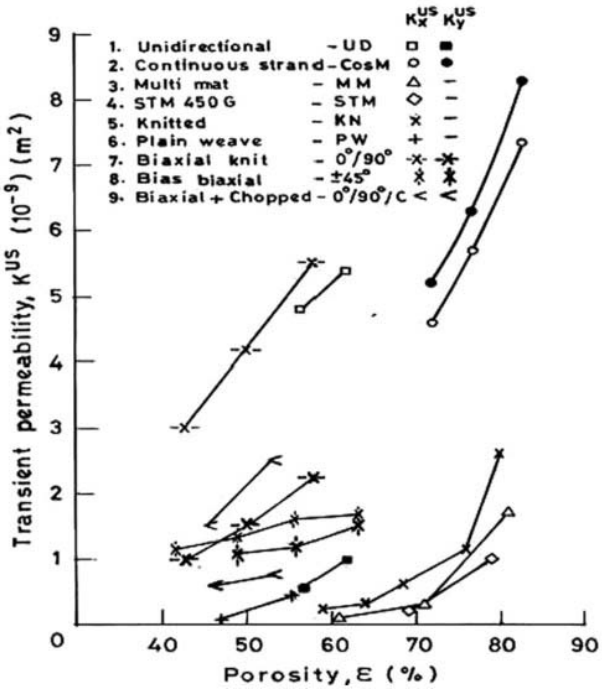

Figure 1.3 Transient permeability as a function of porosity (Naik et al., 2014)

1.4.2.2 Injection Pressure and Vacuum

In RTM or VARTM, injection pressure and vacuum act as the main driving forces for the resin impregnation. Amico and Lekakou (2001) studied the influences of injection pressure on the flow front, and the results show a direct relationship between the injection pressure and the flow front (Figure 1.4). Lekakou et al. (1998) investigated the influence of injection pressure over apparent permeability with the application of Carman-Kozeny equation. And they found its permeability highly depends on both v_f.and fiber tow radius.

Vacuum is often used on its own in VARTM, both injection devices and vacuum assisted are used in most research conducted with RTM. Most vacuum pumps can only provide a pressure differential of 1 bar (100 KPa). In this case, the impact of vacuum is not significant when the injection pressure is high. However, Hyward et al. (1990) studied the effect of vacuum assistance. They observed differences in fiber wetting with or without vacuum; additionally, they proved that the better wetting was not due to cavity pressure differences caused by vacuum. Vacuum reduced the pressure in air-pocket trapped in the interstices of the fiber tows, thus improving the resin penetration.

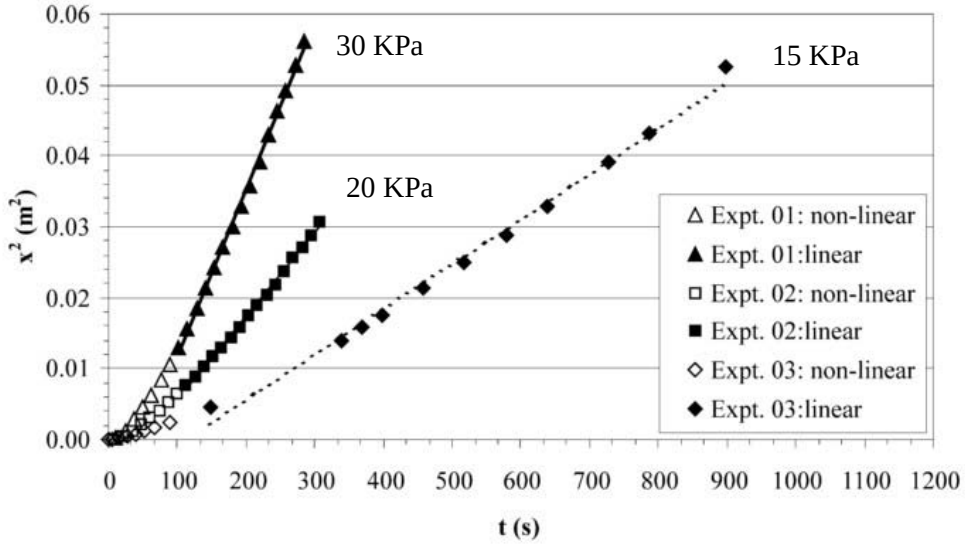

Figure 1.4 Flow front (x2) as a function of the injection pressure at 30, 20 and 15 KPa, respectively (Amico & Lekakou, 2001)

Modeling and predicting the resin flow during impregnation process allows researchers to have an insight into the mechanisms and provides an opportunity to further examine the resin impregnation. Moreover, the resin flow procedure will enable researchers to design the mold shape, location of ports and vents, and set a proper injection pressure and vacuum. In this case, a fundamental understanding of the resin impregnation mechanisms will aid in selection of proper processing parameters, improving quality and reducing cost.

1.5 Research Methods

1.5.1 Response Surface Methodology (RSM)

Response surface methodology (RSM) is a method that can provide researchers with the optimal experimental design by generating significant experiment points, which will effectively reduce the number of trials. In contrast to screening experiments, RSM requires a better understanding of factors that are important to final performance. RSM creates a predictive model of the relationship between the

manually selected factors and the response. This method gives an explicit approximation of the implicit limit state function of the structure through a number of deterministic structural analyses.

1.5.1.1 D-optimal Design

D-optimal design is a computer-aided design based on computer algorithms. It operates by first building an approximate mathematical model or a function to define the relationship between the response (Y) and the independent variables (the factors). Next, the program will generate a set of candidate experimental points based on this model. Finally, the program selects a subset from those points to get the minimized value of $|(X'X)^{-1}|$ matrix (Montgomery, 1997). D-optimal design selects only certain critical points in the complete factorial design that can provide the best estimation without aimless trails. It is efficient for limited replicated experiments due to time or budget.

Because it is a model-dependent design, a model must be established beforehand. Then the computer chooses the optimal set of experimental runs. This set of runs consists of all possible combinations of various factors designed for the experiment.

1.6 Proposed Research

In this research, we are interested in understanding how composite performance varies in terms of different wood strands preforms and resin systems under different processing conditions.

This information is needed as there is a lack of sufficient research on wood strands as reinforcing fibers in composites processed with RTM, required to develop a qualified material for advanced applications.

Thesis is divided into four chapters, including this introductory and literature review chapter. Chapter two and Chapter three address the two objectives presented in this chapter. Chapter two is a complete discussion about influences of parameters in pre-pressing wood strands preform. Chapter three utilizes the conclusion in Chapter two for preform fabrication and then resin impregnation is conducted. Permeability

is estimated and mechanical and physical properties are evaluated. The last chapter, which is Chapter four, summarizes the conclusions of the study, and furthermore, recommendations and future trends are provided based on this study.

This study exhibited great potential for wood strands to be used as reinforcement for wood-based composites using the RTM process. An understanding of the underpinning science and technology of producing wood strand composite products using RTM will be provided. This study is only a beginning of research to be conducted on use of wood strands for value-added applications using industrial scale RTM process.

1.7 References

Advani, S. . G., Bickerton, S., Sozer, E. . M., & Graham, P. . (2000). Fabric structure and mold curvature effects on preform permeability and mold filling in the RTM process. Part I. Experiments. Composites Part A: Applied Science and Manufacturing, 31(5), 423–438. doi:10.1016/S1359-835X(99)00087-1

Amico, S., & Lekakou, C. (2001). An experimental study of the permeability and capillary pressure in resin-transfer moulding. Composites Science and Technology, 61(13), 1945–1959. doi:10.1016/S0266-3538(01)00104-X

Arbter, R., Beraud, J. M., Binetruy, C., Bizet, L., Bréard, J., Comas-Cardona, S., … Ziegmann, G. (2011). Experimental determination of the permeability of textiles: A benchmark exercise. Composites Part A: Applied Science and Manufacturing, 42(9), 1157–1168. doi:10.1016/j.compositesa.2011.04.021

Barraza, H. J., Hamidib, Y. K., Aktasb,, L., O'Rear, E. a., & Altan, M. C. (2004). Porosity Reduction in the High-Speed Processing of Glass-Fiber Composites by Resin Transfer Molding (RTM). Journal of Composite Materials, 38(3), 195–226. doi:10.1177/0021998304038649

Buntain, M. J., & Bickerton, S. (2003). Compression flow permeability measurement: a continuous technique. Composites Part A: Applied Science and Manufacturing, 34(5), 445–457. doi:10.1016/S1359-835X(03)00090-3

Conshohocken, W. (2014). Standard Test Method for Permeability of Rocks by Flowing Air 1, 7–11. doi:10.1520/D4525-08.2

Deacon, B. M. (2012). Mechanical performance of kevlar fabric/carbon nanofiber modified epoxy composites made via vacuum assissted resin transfer molding.

Dong, C. (2006). Development of a process model for the vacuum assisted resin transfer molding simulation by the response surface method. Composites Part A: Applied Science and …, 37(9), 1316–1324. doi:10.1016/j.compositesa.2005.08.012

Ferland, P., & Trochu, F. (1996). Resin Transfer Molding, 17(1).

Fink, B., Hsiao, K., & Mathur, R. (2000). An Analytical Vacuum-Assisted Resin Transfer Molding (VARTM) Flow Model.

Francucci, G., & Vázquez, A. (2012). Capillary effects in vacuum-assisted resin transfer molding with natural fibers. Polymer …. doi:10.1002/pc

Gebart, B., & Lidström, P. (1996). Measurement of in-plane permeability of anisotropic fiber reinforcements. Polymer Composites, 17(1), 43–51.

Gokce, a, Chohra, M., Advani, S., & Walsh, S. (2005). Permeability estimation algorithm to simultaneously characterize the distribution media and the fabric preform in vacuum assisted resin transfer molding process. Composites Science and …, 65(14), 2129–2139. doi:10.1016/j.compscitech.2005.05.012

Haider, M., Hubert, P., & Lessard, L. (2007). An experimental investigation of class A surface finish of composites made by the resin transfer molding process. Composites Science and Technology, 67(15-16), 3176–3186. doi:10.1016/j.compscitech.2007.04.010

Hayward, J., & Harris, B. (1990). The effect of vacuum assistance in resin transfer moulding. Composites Manufacturing. Retrieved from http://www.sciencedirect.com/science/article/pii/095671439090163Q

Hoes, K., Dinescu, D., Sol, H., Vanheule, M., Parnas, R. S., Luo, Y., & Verpoest, I. (2002). New set-up for measurement of permeability properties of fibrous reinforcements for RTM. Composites Part A: Applied Science and Manufacturing, 33(7), 959–969. doi:10.1016/S1359-835X(02)00035-0

Holmberg, J., & Berglund, L. (1997). Manufacturing and performance of RTM U-beams. … Part A: Applied Science and Manufacturing, (97), 513–521.

Khan, R. a., Khan, M. a., Zaman, H. U., Parvin, F., Islam, T., Nigar, F., … Mustafa, a. I. (2011). Fabrication and Characterization of Jute Fabric-Reinforced PVC-based Composite. Journal of Thermoplastic Composite Materials, 25(1), 45–58. doi:10.1177/0892705711404726

Lacovara, B. (1995). Considering Resin Transfer Molding. Composites Fabrication Association S, 1–9.

Lee, G.-W., Lee, N.-J., Jang, J., Lee, K.-J., & Nam, J.-D. (2002). Effects of surface modification on the resin-transfer moulding (RTM) of glass-fibre/unsaturated-polyester composites. Composites Science and Technology, 62(1), 9–16. doi:10.1016/S0266-3538(01)00091-4

Lekakou, C., & Bader, M. G. (1998). Mathematical modelling of macro and micro infiltration in resin transfer moulding (RTM). Comp, 29–37.

Li, Y. (2006). Processing of Sisal Fiber Reinforced Composites by Resin Transfer Molding. Materials and Manufacturing Processes, 21(2), 181–190. doi:10.1081/AMP-200068669

Materials, E., Technique, G., & Ovens, V. (2014). Standard Test Method for Permeability of Thermoplastic Containers to Packaged Reagents or Proprietary Products 1, 1–5. doi:10.1520/D2684-10.2

Montgomery, D. C. (1997). Design and analysis of experiments. Retrieved from

Naik, N. K., Sirisha, M., & Inani, a. (2014). Permeability characterization of polymer matrix composites by RTM/VARTM. Progress in Aerospace Sciences, 65, 22–40. doi:10.1016/j.paerosci.2013.09.002

Parnas, R. S., & Salem, A. J. (1993). A comparison of the unidirectional and radial in-plane flow of fluids through woven composite reinforcements. Polymer Composites, 14(5), 383–394. doi:10.1002/pc.750140504

Rouison, D., Sain, M., & Couturier, M. (2004). Resin transfer molding of natural fiber reinforced composites: cure simulation. Composites Science and Technology, 64(5), 629–644. doi:10.1016/j.compscitech.2003.06.001

Rouison, D., Sain, M., & Couturier, M. (2006). Resin transfer molding of hemp fiber composites: optimization of the process and mechanical properties of the materials. Composites Science and Technology, 66(7-8), 895–906. doi:10.1016/j.compscitech.2005.07.040

Siau, J. F. (1995). Wood--influence of moisture on physical properties. (V. P. I. and S. U. D. of W. S. & F. Products, Ed.). Blacksburg, VA]: Blacksburg, VA : Dept. of Wood Science and Forest Products, Virginia Polytechnic Institute and State University.

Verrey, J., Wakeman, M. D., Michaud, V., & Månson, J. -a. E. (2006). Manufacturing cost comparison of thermoplastic and thermoset RTM for an automotive floor pan. Composites Part A: Applied Science and Manufacturing, 37(1), 9–22. doi:10.1016/j.compositesa.2005.05.048

Chapter 2 Wood strands Preform Architecture Study

2.1 Introduction

In a resin transfer molding (RTM) operation, preform is the fiber mat loaded into the mold cavity prior to injecting with resin. Preform quality is very important to the performance of composite products. Preform used in RTM varies from woven fibers like glass fiber (Barraza et al.; Kim, and Daniel; Francucci and Vázquez) and natural fibers (Francucci & Vázquez, 2012; Mariatti, Jannah, Abu Bakar, & Khalil, 2008; Rouison, Sain, & Couturier, 2004) to non-woven random fibers (Zhang, Comas-Cardona, & Binetruy, 2012; Zhang, Cosson, Comas-Cardona, & Binetruy, 2011). For non-woven random fibers, architecture and handling characteristics are of vital importance to the resin injection. However, lots of researchers placed the fiber inside the mold and apply pressure and inject resin simultaneously (Sawpan, Pickering, & Fernyhough, 2012), which makes it difficult to control the preform quality.

Traditionally, trial-and-error methods are widely applied in the composite industry, but are very costly and time consuming. Also the performance and consistency of this kind of methods highly depends on the operator. The method used in this research is optimal design, using design of experiment (DOE), creation of response surface for each variables and optimization (Dong, 2006; Nordlund & Michaud, 2012). DOE identifies the significant processing variables and finds a suitable approximation for the true functional relationship between response and the set of independent variables. First-order or second-order model with response surface methodology (RSM) can be developed, providing overall information of the effects on the processing variables. Optimization procedure finds the optimized response by specifying criterion and then chooses the design points from a set of candidate points (Montgomery, 1997).

2.2 Objective

The objective of this study is to study the influence of wood strands preform architecture on the RTM process for suitable preform fabrication. The specific tasks to achieve this objective are to:

1. Determine the significant processing variables using the design of experiments (DOE).
2. Evaluate the preform performance including handling property, void volume and actual density with different values of target density, cold-set resin (PVAc) content to maintain preform integrity during handling and processing, and pre-pressing duration.

2.3 Experiment of Preform Fabrication

2.3.1 Design of Preform Fabrication

Three processing variables were considered in designing the experiment to evaluate their influence on quality of end product produced. They are consolidated panel target density, PVAc resin content, and pre-pressing duration. The ranges of each variable were chosen based on past research on oriented strand board (OSB) (Han, Wu, & Lu, 2006), recommendations of adhesive suppliers, and some preliminary experiments. The factors considered in designing the experiment and constraints placed on them are shown in Table 2.1. D-optimal design was used to generate 20 experimental design points (Table 2.2). Handling, which describes the ease of handle, void volume in preform and actual density were three responses evaluated.

Table 2.1 Lower and upper constraints for each of the processing variables in determining experimental design points using DOE.

Processing variable	Low	High
Target density (kg m^{-3})	481	801
PVAc content (%)	2	6
Pre-pressing duration	400	600

Table 2.2 Experimental design points for response model.

	Processing variables		
Run #	Density kg m^{-3}	PVAc content %	Pre-pressing duration s
1	480	2	600
2	480	3.42	300
3	576	4.28	428
4	801	6	600
5	801	6	600
6	480	2	600
7	801	4.38	422
8	769	2.36	450
9	687	6	300
10	608	2	422
11	480	6	300
12	480	6	495
13	610	4.4	600
14	684	6	471
15	801	2	300
16	801	4.38	422
17	801	2	600
18	801	2	600
19	801	2	300
20	689	3.76	300

2.3.2 Experimentation of Preform Fabrication

2.3.2.1 Materials

PVAc adhesive, Assembly 161 (Franklin International, Inc), and hybrid poplar wood strands (moisture content of 3.5%) were used in conducting this study on preform characteristics.

2.3.2.2 Experimental Procedure

Wood strands were sprayed with desired PVAc resin (based on the run number and the corresponding resin level suggested by the DOE) with an air gun prior to forming in a bag. A strand mat was then formed and pre-presses as shown in Figure 2.1. Metal vanes spaced 25-mm apart (Figure 2.1a) help in orienting the strands with respect to the long axis of the mat. The thickness control pre-press schedule is shown in Table 2.3, and its corresponding pressure is shown in Figure 2.2. To ensure a proper compression for the wood strand preform, the mold was closed gradually such as it took 10 s to go from 5.38 mm to 3.81 mm. And then hold at the preform target thickness for 300 to 600 s based on Table 2.2. A typical pre-pressed preform that is ready to be trimmed and placed in the RTM mold is shown in Figure 2.3. The required size of the preform used in RTM was designed to be 305x305 mm^2, so the size of the forming box was 381x381 mm^2 to provide enough space for trimming, ensuring a uniform preform after trimming (Figure 2.3). Preforms were conditioned for 24 hours in 20 °C, 65% relative humidity, 12 % equilibrium moisture content.

a) b) c)

Figure 2.1 Forming of strand mat (a), formed mat (b), and mat pre-pressing (c).

Table 2.3 Thickness control pre-press schedule for preform fabrication.

Time (s)	Thickness (mm)
10	From 0.212 to 0.150
10	From 0.150 to 0.125
300-600	0.125 (preform target thickness)
	Press open

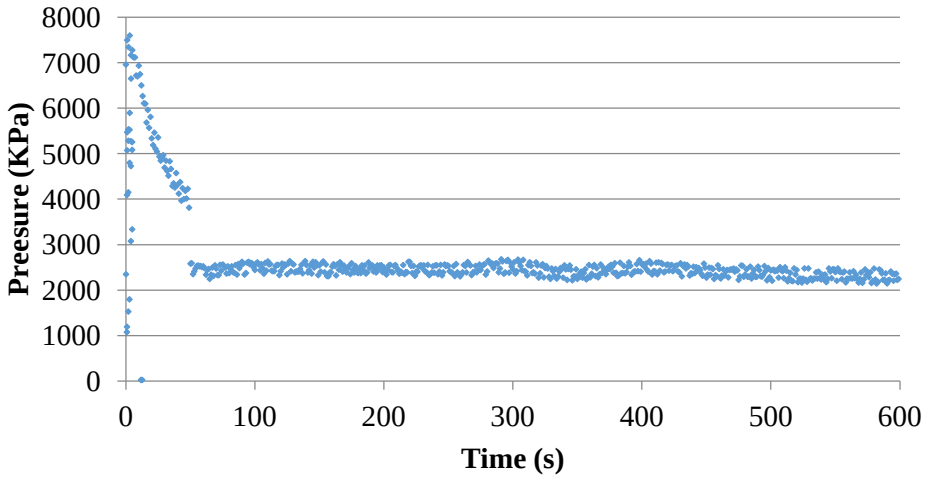

Figure 2.2 A typical pressure profile for pre-pressing a preform.

a) b)

Figure 2.3 a) Preform after pre-pressing, b) after trimming (305x305 mm²).

2.3.3 Evaluation Methods of Preform Quality

2.3.3.1 Handling

Handling describes the visual inspection of the preform quality, which was assigned a rating of 1 to 4 depending on its level of integrity -- bad, fair, good, or excellent. Following is a qualitative description of the preform based on the rating.

Bad (1): Preforms are unable to handle, obvious surface and edge voids, bad bonding or uneven thicknesses observed.

Fair (2): Preforms are unable to handle, bad bonding but less obvious surface and edge voids observed.

Good (3): Preforms are able to handle with strands well bonded together, but thickness is uneven.

Excellent (4): Preforms are able to handle with strands well bonded together, and good surface quality.

2.3.3.2 Void Volume

Void volume quantifies the sum of all the voids, macro- and micro-voids, within the preform. They defined the macro-voids as the voids between the fiber tows (in this case wood strands), and the micro-voids are voids within the fiber tows (Chan & Morgan, 1993; Francucci & Vázquez, 2012; Ruiz, Achim, Soukane, Trochu, & Breard, 2006). For a wood strands mat, micro-voids are the voids in the wood cells or lumens. And macro-voids are the interstitial spaces between strands. The voids considered in this study are the total voids including both micro- and macro-voids, which can be calculated using the estimated cell wall specific gravity of wood fiber, which is approximately 1500 kg m^{-3} (Forest Products Laboratory, 2010). Equation 2.1 and Equation 2.2 were used to calculate the void volume.

$$m_{preform} = m_{fiber} + m_{PVAc} \quad \text{Equation 2.1}$$

$$V_v = \frac{v_{preform} - \frac{m_{fiber}}{\rho_{cell\ wall}} - \frac{m_{PVAc}}{\rho_{PVAc}}}{v_{preform}} \quad \text{Equation 2.2}$$

where, m_{resin} is the weight of actual PVAc resin sprayed onto the wood strands, m_{fiber} is the weight of wood strands based on the target density, the ρ_{PVAc} is 1060 kg m^{-3}, and $\rho_{cell\ wall}$ is 1500 kg m^{-3}.

The preform volume ($v_{preform}$) consists of fiber volume (v_{fiber}), PVAc volume (v_{PVAc}) and void volume (v_{void}). Preform volume is the volume based on target thickness. Void volume was calculated by subtracting fiber volume and PVAc volume (Equation 2.1). Knowing the mass weight and density of fiber and PVAc, void volume percentage (V_v) can then calculated by dividing by the preform volume (Equation 2.2).

2.3.3.3 Actual Density

Actual density of the preform is the density after the preform was taken out of the press, and is measured based on its thickness measured 24-hrs after pre-pressing the mat. Thickness was measured at five

different points as illustrated in Figure 2.4. Target density is a desired goal; nevertheless, it cannot be reached by pre-pressing at room temperature.

Figure 2.4 Thickness measurement of a preform.

2.4 Results and Discussions

2.4.1 Handling

Difference in the classification of preforms based on their level of handling is shown in Figure 2.5. An analysis of variance (ANOVA) was performed to examine statistical significance of the processing factors on the ability for handling preforms after pre-pressing. The ANOVA table (Table 2.4) shows that target density and PVAc content are significant variables. A linear model estimating the relationship between handling, target density and PVAc content was then established in Equation 2.3 with coefficients shown in Table 2.5. Its corresponding response surface is illustrated in Figure 2.6.

Handling property improves from 1 to 4 when increasing both target density and PVAc content. Note that the best handling appears with the highest target density and highest PVAc content. Likewise, the worst handling arises with the lowest target density and lowest PVAc content. As expected, higher target density and more resin lead to better bonding among the strands and allow for better handling of the preform.

a) Handling level 1

b) Handling level 2

c) Handling level 3

d) Handling level 4

Figure 2.5 Handling properties of preform: a) poor, b) fair, c) good, and d) excellent.

Table 2.4 AVOVA for handling property.

Source	Sum of Squares	df	Mean Square	F-value	p-value
Model	10.8332	6	1.8055	3.3934	0.0307*
A-Target density	3.0372	1	3.0372	5.7083	0.0327*
B-PVAc	2.6873	1	2.6873	5.0507	0.0426*
C-Pre-pressing duration	0.0469	1	0.0469	0.0881	0.7713
A:B	1.7156	1	1.7156	3.2244	0.0958
A:C	0.4050	1	0.4050	0.7613	0.3988
B:C	0.4626	1	0.4626	0.8694	0.3681
Residual	6.9168	13	0.5321		
Lack of Fit	4.4168	8	0.5521	1.1042	0.4782
Pure Error	2.5	5	0.5		
Cor Total	17.75	19			

* Significant Variable or interaction

Table 2.5 Fitted linear regression model coefficient for handling.

Factor	Intercept	A-Target density	B-PVAc content
Coefficient	-0.4999	3.1873E-3	0.2808

$$Y_{Handling} = -0.4999 + 3.1873E-3 \times A + 0.2808 \times B \quad \text{Equation 2.3}$$

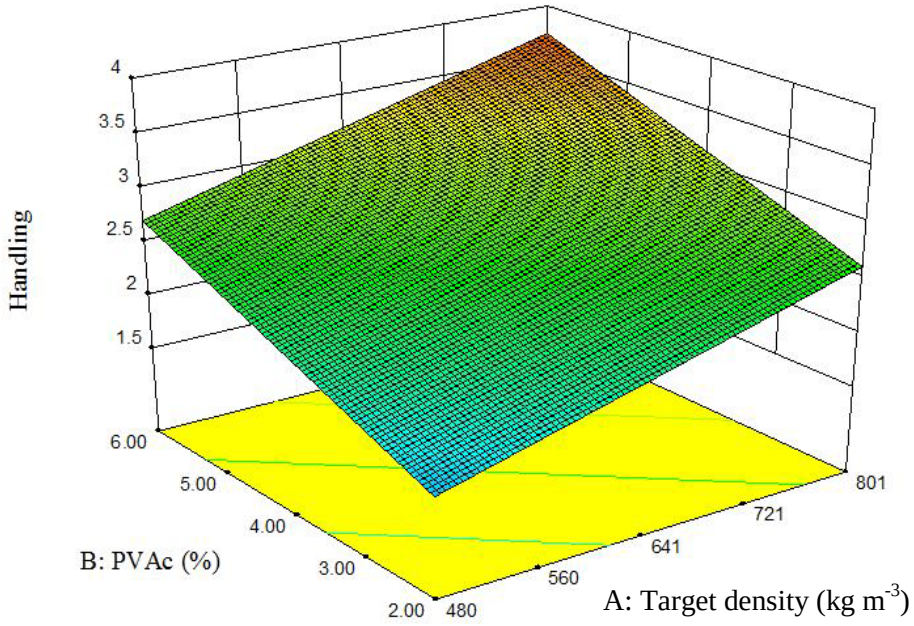

Figure 2.6 Response surface of the fitted linear regression model for handling.

2.4.2 Void Volume

The ANOVA (Table 2.6) for void volume indicates the PVAc content and the interaction between target density and PVAc content are significant variables. A modified model with significant terms estimating the relationship between void volume, target density and PVAc content was then established in Equation 2.4 with coefficients shown in Table 2.7. Its corresponding response surface is illustrated in Figure 2.7.

Results show a significant decrease in void volume (from 0.83 to 0.75) by increasing PVAc content from 2% to 6% at 801 kg m^{-3} target density, or by increasing target density from 480 to 801 kg m^{-3} at 6% PVAc content (Figure 2.8). However, void volume does not follow this trend at lower target density or PVAc content. At lower PVAc content, mats pressed to higher densities tend to springback, thus increasing void volume post pre-pressing. The linear regression for experimental void volume as a function of PVAc content is illustrated in Figure 2.8, which shows that void volume is inversely proportional to the PVAc content. This is because higher PVAc content generates better bonding among wood strands, resulting in less thickness recovery.

Umer et al. (2007) studied the fiber volume fraction of the pine fiber mat, which is the only research published utilizing wood fiber in RTM. Wood was reduced into fiber form similar to in a fiberboard manufacturing plant. They achieved a fiber volume fraction of 0.13-0.14 and suggested that with full vacuum utilized in resin infusion technology, a fiber volume fraction of 0.25-0.26 can be achieved. As for the synthetic fibers, such as glass fibers, in the RTM process, typical fiber volume fraction ranges from 0.25-0.50 (Zhang et al., 2012). Roy et al. (2007) used the carbon fiber with porosity of 86.6% to estimate the 1-D flow permeability. Therefore, a fiber volume fraction of 0.17 to 0.25 could be efficient in resin transfer for wood strand preforms studied in this research.

Table 2.6 AVOVA for void volume.

Source	Sum of Squares	df	Mean Square	F-value	P-value
Model	130.92	6	21.82	11.98	0.0001*
A-Target density	7.11	1	7.11	3.90	0.0698
B-PVAc	39.51	1	39.51	21.70	0.0004*
C-Pre-pressing duration	0.85	1	0.85	0.46	0.5073
A:B	27.66	1	27.66	15.19	0.0018*
A:C	0.38	1	0.38	0.21	0.6550
B:C	6.03	1	6.03	3.31	0.0918
Residual	23.67	13	1.82		
Lack of Fit	12.18	8	1.52	0.66	0.7123
Pure Error	11.49	5	2.30		
Cor Total	154.59	19			

* Significant Variables or interaction

Table 2.7 Fitted regression model coefficients for void volume.

Factor	Intercept	A-Target density	B-PVAc content	A:B
Coefficient	75.3527	0.0142	2.2677	-5.2419

$$Y_{Void\ volume} = 75.3527 + 0.0142 \times A + 2.2677 \times B - 5.2419 \times A \times B \quad \text{Equation 2.4}$$

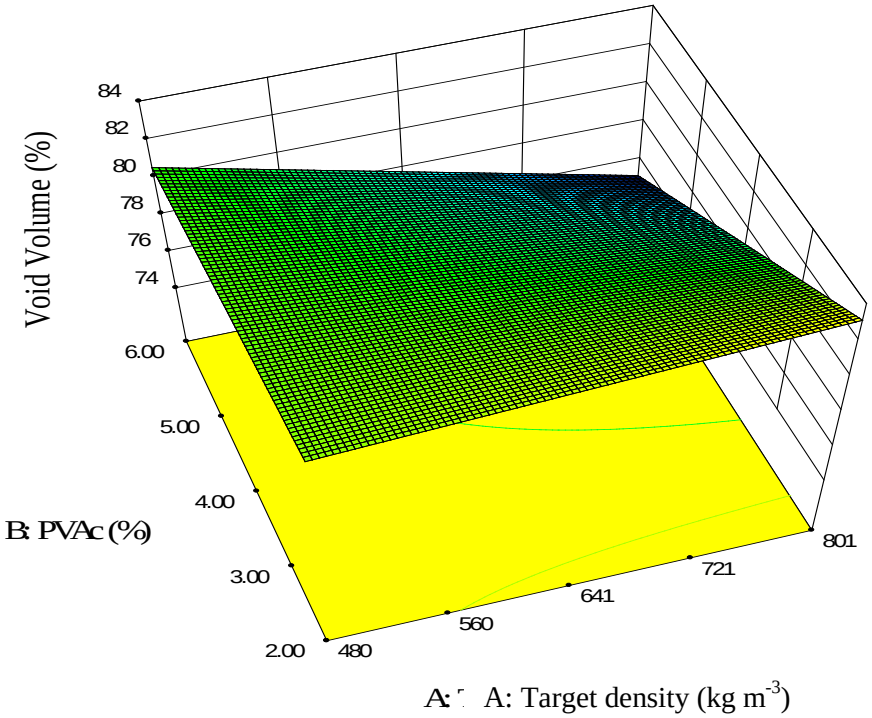

Figure 2.7 Response surface of the fitted regression model for void volume.

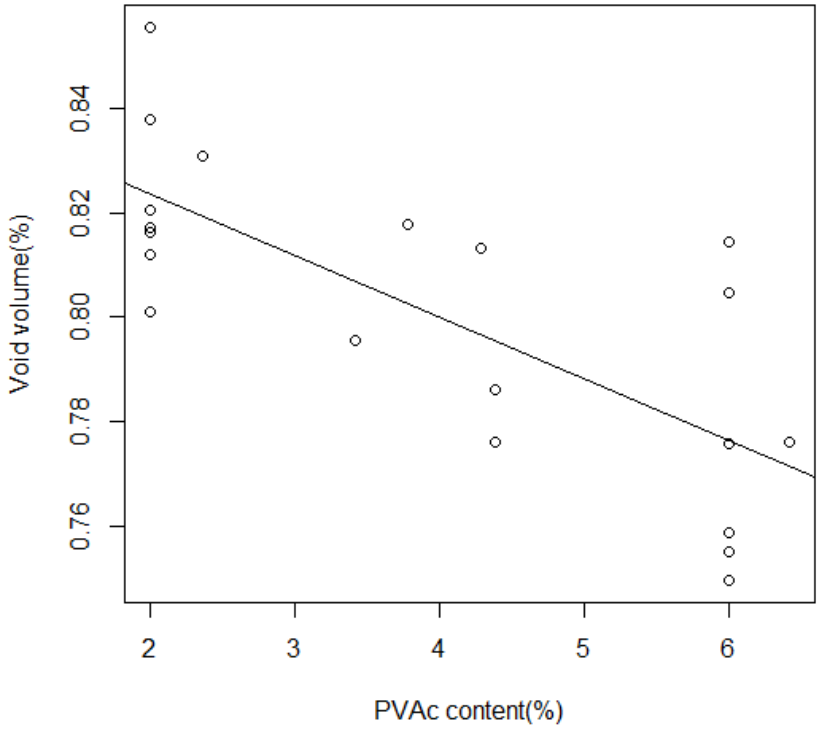

Figure 2.8 Void volume as a function of PVAc content (experimental points).

2.4.3 Actual Density

P-values in ANOVA table (Table 2.8) demonstrate that PVAc content and the interaction term of target density and PVAc content are significant. The modified model with significant terms estimating the relationship between actual density and PVAc content and target density was then shown in Equation 2.5 with coefficients in Table 2.9. The corresponding response surface was shown in Figure 2.9.

The statistical analysis indicates no significant variation in actual density when target density varies. This can be proved by stable response surface graph at very low PVAc content shown in Figure 2.9. Moreover, actual density increases with increased target and increased PVAc content, though not dramatically (from 304 to 336 kg m^{-3}) (Figure 2.7). Notice that this trend becomes more apparent under high PVAc content. Again, adhesive (PVAc resin) plays a vital role in bonding strands in the preform and maintaining a

thickness close to the target thickness mat was pre-pressed to reach target density. An increasing trend for experimental points of actual density (Figure 2.8) as PVAc content increases shows agreement with the estimated model. Results show the importance of PVAc content in maintaining the preform quality prior to being molded using RTM process; resin content is extremely crucial to mold higher density panels.

Umer et al. (2007) have also encountered the springback after wood fiber preform pre-pressing. Mat was pressed as close to the final thickness as possible to achieve good packing. Their fiber density was assumed to be 1500 kg m^{-3}, however, the actual density varied from 350-2100 kg m^{-3} based on the manufacturing methods.

Table 2.8 AVOVA for actual density

Source	Sum of Squares	df	Mean Square	F-value	P-value
Model	23347	6	3891	10.2193	0.0003*
A-Target density	1438	1	1439	3.7783	0.0739
B-PVAc	5915	1	5916	15.5366	0.0017*
C-Pre-pressing duration	201	1	201	0.5272	0.4807
A:B	5881	1	5881	15.4447	0.0017*
A:C	92	1	92	0.2420	0.6310
B:C	1253	1	1253	3.2904	0.0928
Residual	4950	13	381		
Lack of Fit	2457	8	307	0.6162	0.7418
Pure Error	2493	5	498		
Cor Total	28298	19			

* Significant Variable or interaction

Table 2.9 Fitted regression model coefficients for actual density.

Factor	Intercept	A-Target density	B-PVAc content	A:B
Coefficient	366.804	-0.2079	-35.0424	0.0761

$$Y_{Actual\ density} = 366.804 - 0.2079 \times A - 35.0424 \times B + 0.0761 \times A \times B$$ Equation 2.5

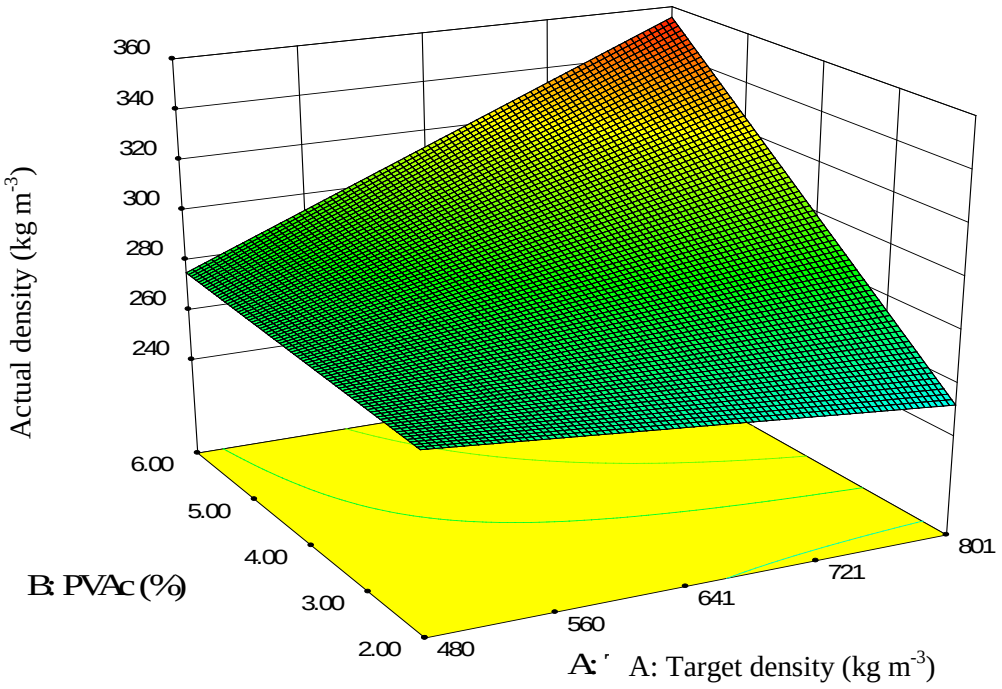

Figure 2.9 Response surface of actual density vs. target density and PVAc content.

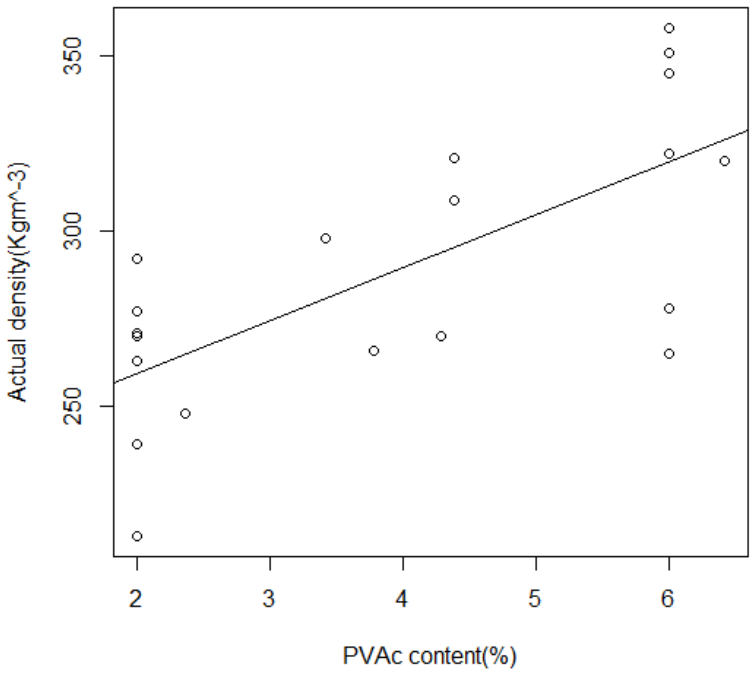

Figure 2.10 Actual density vs. PVAc content (experimental points).

2.5 Optimization

Results, as expected, show that there is a fine balance between target density and PVAc content to ensure good preform handling prior to molding and achieve necessary void space for resin penetration. Based on the regression equations, an optimization procedure was carried out by RSM to determine appropriate processing variables for a good handling, good integrity with sufficient void volume preform characteristics. A longer pre-press duration of 600 seconds for preform fabrication is maintained as no significant difference was found within the range from 300 to 600 seconds. Design-Expert ® provides several solutions within the boundary of constraints (Table 2.10). Aiming at a higher target density and keeping the PVAc content at 6%, it shows a high experimental desirability (0.950) with almost perfect handling (Table 2.11).

The processing variables including PVAc content and pre-pressing duration will be used in the preform fabrication for the resin flow study and mechanical performance study in Chapter 3.

Table 2.10 Constraints and their goals in optimization for preform fabrication.

Name	Goal	Lower limit	Upper limit	Importance
Target density	in range	480	801	3
PVAc content	=6	2	6	3
Pre-pressing duration	=600	300	800	3
Handling	maximize	1	4	5
Void volume	minimize	0.7497	0.8554	3
Actual Density	maximize	213	358	3

Table 2.11 Optimization solution for preform fabrication.

Target density kg m^{-3}	Pre-pressing duration s	Handling	Void volume %	Actual density kg m^{-3}	Desirability
801	600	3.7379	75.15	355	0.950

2.6 Conclusions & Recommendations

The main objective of this part is to determine the significant preform architecture variables and to evaluate the preform performance including handling property, void volume and actual density with different values of target density, cold-set resin (PVAc) content to maintain preform integrity during handling and processing, and pre-pressing duration. The analysis was conducted with both experimental evaluation and RSM models. Pre-pressing duration is not a significant variable in this study; however, it could depend on the species and the type of resin being used..

Target density and PVAc are both significant variables to handling property. Moreover, handling performance increases with an increase in target density and PVAc content. PVAc content is critical in

achieving and maintaining higher density preforms and controlling the void content necessary for resin penetration.

Since the preform is made for a mold with constant depth, the desired preform requires constant horizontal density, acceptable level of density for good resin penetration, and acceptable product densities with good quality surfaces. A strategy of trimming the preform prior to pre-pressing is applied to meet those requirements. And this strategy will be applied in the subsequent resin flow study.

2.7 References

Barraza, H. J., Hamidib, Y. K., Aktasb,, L., O'Rear, E. a., & Altan, M. C. (2004). Porosity Reduction in the High-Speed Processing of Glass-Fiber Composites by Resin Transfer Molding (RTM). Journal of Composite Materials, 38(3), 195–226. doi:10.1177/0021998304038649

Chan, A., & Morgan, R. (1993). Tow impregnation during resin transfer molding of bi-directional nonwoven fabrics. Polymer Composites, 14(4), 335–340.

Dong, C. (2006). Development of a process model for the vacuum assisted resin transfer molding simulation by the response surface method. Composites Part A: Applied Science and …, 37(9), 1316–1324. doi:10.1016/j.compositesa.2005.08.012

Forest Products Laboratory. (2010). Wood Handbook: Wood as an Engineering Material. Agriculture (Vol. 72, p. 466). doi:General Technical Report FPL-GTR-190

Francucci, G., & Vázquez, A. (2012). Capillary effects in vacuum-assisted resin transfer molding with natural fibers. Polymer …. doi:10.1002/pc

Han, G., Wu, Q., & Lu, J. Z. (2006). SELECTED PROPERTIES OF WOOD STRAND AND ORIENTED STRANDBOARD FROM SMALL-DIAMETER SOUTHERN PINE TREES 1, 38(4), 621–632.

Kim, S. K., Kim, D.-H., & Daniel, I. M. (2003). Optimal control of accelerator concentration for resin transfer molding process. International Journal of Heat and Mass Transfer, 46(20), 3747–3754. doi:10.1016/S0017-9310(03)00214-X

Mariatti, M., Jannah, M., Abu Bakar, a., & Khalil, H. P. S. a. (2008). Properties of Banana and Pandanus Woven Fabric Reinforced Unsaturated Polyester Composites. Journal of Composite Materials, 42(9), 931–941. doi:10.1177/0021998308090452

Montgomery, D. C. (1997). Design and analysis of experiments.

Nordlund, M., & Michaud, V. (2012). Dynamic saturation curve measurement for resin flow in glass fibre reinforcement. Composites Part A: Applied Science and Manufacturing, 43(3), 333–343. doi:10.1016/j.compositesa.2011.12.001

Rouison, D., Sain, M., & Couturier, M. (2004). Resin transfer molding of natural fiber reinforced composites: cure simulation. Composites Science and Technology, 64(5), 629–644. doi:10.1016/j.compscitech.2003.06.001

Roy, T., Tan, H., & Pillai, K. M. (2007). A Method to Estimate the Accuracy of 1-D Flow Based Permeability Measuring Devices. Journal of Composite Materials, 41(17), 2037–2055. doi:10.1177/0021998307074109

Ruiz, E., Achim, V., Soukane, S., Trochu, F., & Breard, J. (2006). Optimization of injection flow rate to minimize micro/macro-voids formation in resin transfer molded composites. Composites Science and Technology, 66(3-4), 475–486. doi:10.1016/j.compscitech.2005.06.013

Sawpan, M. a., Pickering, K. L., & Fernyhough, a. (2012). Analysis of mechanical properties of hemp fibre reinforced unsaturated polyester composites. Journal of Composite Materials, 47(12), 1513–1525. doi:10.1177/0021998312449028

Umer, R., Bickerton, S., & Fernyhough, a. (2007). Characterising wood fibre mats as reinforcements for liquid composite moulding processes. Composites Part A: Applied Science and Manufacturing, 38(2), 434–448. doi:10.1016/j.compositesa.2006.03.003

Zhang, F., Comas-Cardona, S., & Binetruy, C. (2012). Statistical modeling of in-plane permeability of non-woven random fibrous reinforcement. Composites Science and Technology, 72(12), 1368–1379. doi:10.1016/j.compscitech.2012.05.008

Zhang, F., Cosson, B., Comas-Cardona, S., & Binetruy, C. (2011). Efficient stochastic simulation approach for RTM process with random fibrous permeability. Composites Science and Technology, 71(12), 1478–1485. doi:10.1016/j.compscitech.2011.06.006

Chapter 3 RTM of Hybrid Poplar Wood Strand Composite Panels: Resin Flow and Property Analysis

3.1 Introduction

Liquid composite molding (LCM), which includes rein transfer molding (RTM) and vacuum assisted resin transfer molding (VARTM), has emerged as a cost-effective method for manufacturing glass or carbon fiber reinforced polymer composite materials in automobile and aerospace industries. Besides synthetic fibers, some natural fibers including jute, sisal and flax have also been researched in producing composites panels with RTM or VARTM (Hossain, Islam, Vuurea, & Verpoest, 2013; Khan et al., 2011; Li, 2006) for potential applications as door and interior paneling in the automobile industry. Generally, they have found that natural fiber reinforced composites made with RTM exhibit higher tensile and flexural properties when compared with compressed molded composites (Idicula, Sreekumar, Joseph, & Thomas, 2009; Li, 2006). Mechanical properties are found to be linear with fiber volume fraction. Unsaturated polyester, vinyl ester and epoxy are the most commonly used thermosetting resins for RTM. Additives are not widely used with resin, however low profile additives (LPA) used for shrinkage control was analyzed by some researchers (Haider, Hubert, & Lessard, 2007).

Wood composite industries have been utilizing wood strands for manufacturing hot pressed composite products such as oriented strand board (OSB) and laminated strand lumber (LSL) for building and furniture applications. Umer et al. (2007) studied use of pine fibers as reinforcement in RTM. Fibers were produced using typical processes used in pulp production. However, wood strands as reinforcing fibers have never been evaluated with RTM or VARTM. Wood strands offer an opportunity to produce stronger and stiffer composite panels compared to wood fibers or particulates.

Resin flow through a preform during the molding process is one of the key factors in determining the quality and performance of the composite panels produced using the RTM technology. Resin flow

influences fill time, quality of the surface, voids in the end product, and composite product performance. Permeability of the preform determines the resin flow. Permeability of a wood strand preform is determined by the bulk movement of the resin through the interstitial spaces among the strands, capillary action through the fiber lumens in the strands, and diffusion through the cell walls of the fibers (Siau, 1995). Therefore, preform architecture defined by its density, element dimensions and orientation, resin flow properties (such as viscosity and molecular weight), injection pressure and vacuum can all have a huge impact on the resin flow behavior. Researchers to estimate preform permeability often use Darcy's law and Carman-Kozeny equations. Past work has shown a decreasing trend with increasing fiber volume fraction (Pomeroy, 2009). Moreover, natural fibers tend to have lower permeability than synthetic fibers for more than 2 orders of magnitudes (Lee et al., 2002; Umer et al., 2007) due to the tendency of natural fibers to absorb fluid, which increases the flow resistance. A good understanding of resin flow property through a preform of discontinuous elements is necessary for manufacturing wood strand composite panels of acceptable quality and performance for automobile and aerospace industries.

The focus of this study is to characterize the resin flow behavior through hybrid poplar strand preforms, examine the influence of resin flow on panel performance (mainly flexure behavior), and establish benchmark values for important physical and mechanical properties of the composite panels produced using RTM. Resin flow analysis was also used to indirectly estimate permeability by three different methods. Influence of preform density, resin viscosity, and pressure, on preform permeability and panel performance was investigated. Preform was pre-pressed and inserted into a matched metal mold for resin injection and curing. The depth of mold cavity determined the thickness of composite panels. However, when using a transparent mold top for resin flow visualization, the deformation of the mold top is inevitable, which alters the compression of fiber preform. Deflections at the center are much larger than on the edges of the mold. Gebart et al (1996) reported that at approximately 3 bar (300 KPa) of pressure, the deflection at the center was close to 1 mm for an 800×800×3 mm mold. Some researchers focused on compression driven flow (Bickerton & Abdullah, 2003; Buntain & Bickerton, 2003) instead of pressure

driven flow. The advantage is permeability can be measured continuously over a wide range of fiber volume fraction in a single efficient test. Thickness of panels can be well controlled, which ensures an accurate fiber volume fraction. Instead of taking compression into consideration, vacuum level was quantified in this study as it was the only factor responsible for preform compression under constant clamping force.

3.2 Objective

The primary objective of this study is to analyze the influence of RTM processing parameters on a composite panel quality and performance, and develop benchmark performance values for wood strand composite panels produced using the RTM process. The specific tasks to achieve the objective are to:

1. Investigate the influence of preform density, injection pressure, vacuum, and resin viscosity on the resin flow behavior, including permeability, surface voids and flexural properties of molded wood strand composite panels.
2. Evaluate mechanical and dimensional stability properties of composite panels produced with three different resin systems.

3.3 Methodology

Study was conducted in two phases to meet the objectives. In the first phase, resin flow analysis was conducted to estimate preform permeability (in this study it refers to specific permeability K). Additionally, influence of preform porosity on specific permeability was examined. A relationship between RTM processing factors and end panel performance was also evaluated. Influence of processing factors, including preform density, resin injection pressure, vacuum, and resin viscosity, was evaluated on the performance of composite panel produced. Performance metrics were area of surface voids and composite panel flexural properties, namely modulus of rupture (MOR) and modulus of elasticity (MOE). Based on the first phase of the study, an injection pressure, vacuum and preform density were chosen and

held constant in manufacturing composite panels. However, three resin types with different mechanical properties and viscosities (Table 3.1) were used in examining their influence on panel properties. Panel properties evaluated were MOR and MOE in bending, tensile strength and modulus, internal bond strength (IB), water absorption and thickness swell.

Table 3.1 Resin systems used in resin flow study and panel performance analysis (Resin Technical data sheet).

Resin type	Styrene monomer (wt %)	Cobalt[a] (wt %)	Cobalt[b] (wt %)	Cobalt[c] (wt %)	Density (kgm^{-3})	Dynamic viscosity (cP)	MOR (MPa)	MOE (GPa)	Tensile Strength (MPa)	Tensile Modulus (GPa)
Unsaturated polyester	37.74	0.0420	0.1820	NA	1091	90	110	4.07	59	4.0
Bisphenol-A based vinyl ester	48.37	0.0180	0.1260	NA	1028	100	152	3.45	83	3.7
Epoxy vinyl ester	45.00	NA	NA	0.3	1046	370	152	3.38	83	3.2

[a] Cobalt neodecanoate, 26% cobalt
[b] Cobalt[2] 2-ethylhexanoate, 12% cobalt
[c] Cobalt[3]-naphthenate, 53% in mineral spirits

3.3.1 Experimentation of Resin Flow and Influence of Processing on Panel Performance

3.3.1.1 Resin Flow Analysis

The processing variables and their lower and upper levels selected to analyze the resin flow are shown in Table 3.2.Note that injection pressure and vacuum varied from lower to upper constraints continuously. However, three levels of resin viscosity and preform density were chosen to be examined. The levels of independent variables were chosen based on the existing literature (Ferland & Trochu, 1996; Naik et al., 2014) and preliminary work. A D-optimal design based on response surface methodology (RSM) was

used to obtain design runs (Table 3.3). Influence of preform characteristics and resin properties on permeability estimated using three methods was evaluated. Responses measured to quantify the performance were panel surface voids and composite panel modulus of elasticity and rupture.

Table 3.2 Lower and upper constraints for each of the processing variables in design of experiment for resin flow study.

Variables	Name	Units	Minimum	Maximum
A	Injection pressure	KPa	34	241
B	Vacuum	KPa	34	91
C	Resin viscosity	cP	90	370
D	Preform density	kg m^{-3}	320	640

Table 3.3 Experimental design points recommended by DOE for the resin flow study.

Run	Processing variables			
	A:Injection pressure	B:Vacuum	C:Resin viscosity	D:Preform density
	KPa	KPa	cP	kg m^{-3}
1	131	34	135	641
2	193	47	135	481
3	241	61	90	641
4	145	85	90	320
5	241	81	370	320
6	38	34	90	481
7	34	88	370	641
8	103	71	135	481
9	34	88	370	320
10	48	54	135	641
11	117	34	135	320
12	38	34	90	481
13	241	88	370	641
14	241	41	370	641
15	241	34	370	641
16	138	71	370	481
17	241	34	90	320
18	241	25	135	481
19	241	18	90	641
20	34	25	90	641
21	241	24	370	320
22	34	18	135	320
23	165	25	135	641
24	41	10	370	320
25	34	25	370	320

The top half of the mold used in the RTM process for resin flow analysis was made of acrylic and transparent (Figure 3.1a). Vacuum pump was connected to a resin trap that was directly attached to the outlet port. A 2100cc Pneumatic RTM Injection System from Radius (Appendix A) was used for resin injection. Two clear films were laid on both the inner surfaces of the cavity to provide fine finish; these films also help during the de-molding process. A critical requirement for the RTM process is an airtight mold. Sealant (Figure 3.1b) and rubber sponge cord gasket seal were used to provide high tack between the two mold halves (Figure 3.1c). Four metal strips and eight C-clamps were used to ensure uniform pressure over the four edges. A schematic of the experimental setup is illustrated in Figure 3.1d.

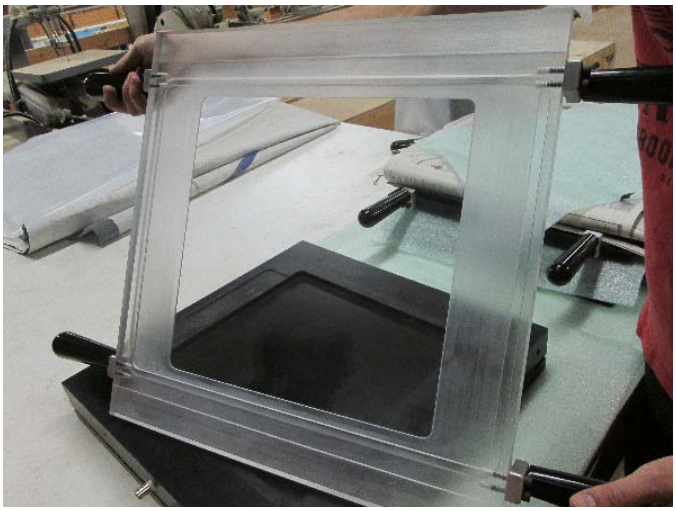

a) Transparent mold top made with acrylic

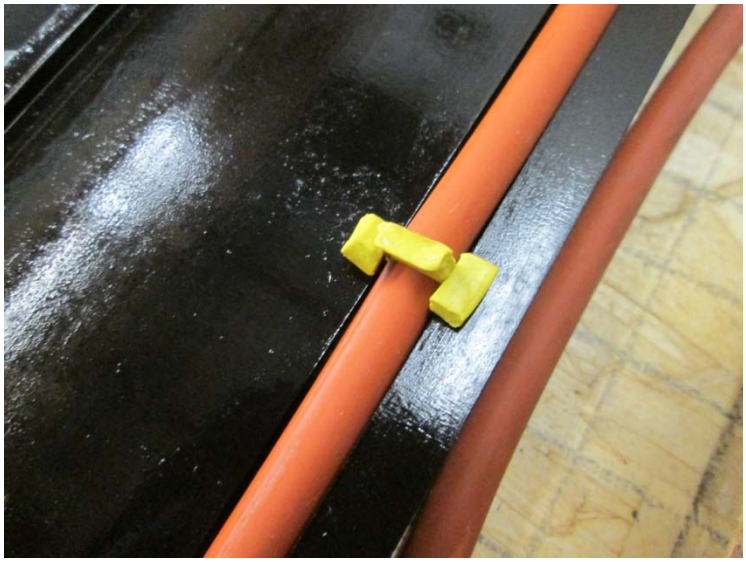

b) Sealant tape applied to provide seal for the mold

c) Rubber sponge cord gasket seal inside the mold groove

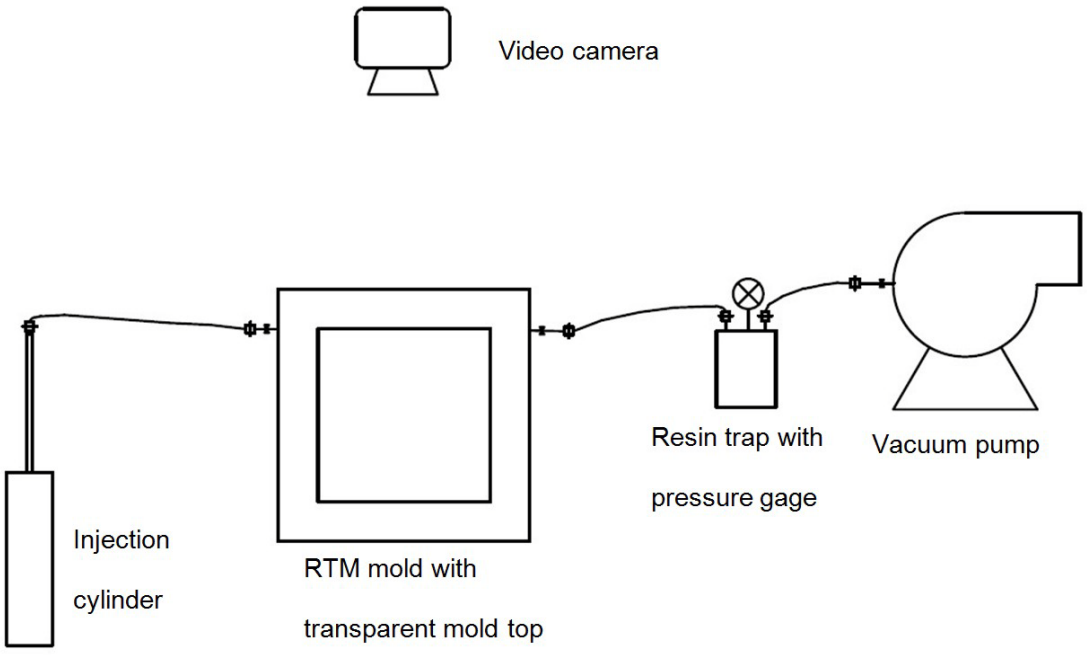

d) A schematic of the experimental setup

Figure 3.1 Transparent mold top and experimental setup for resin flow analysis.

Three types of resins used in this study are listed in Table 3.1. Unsaturated polyester and bisphenol-A based vinyl ester were from CCP Composites, and epoxy vinyl ester was from Ashland. Release agent MR 515 was supplied by ChemTrend. The resins and release agent were used without any further treatment. 1% methyl ethyl ketone peroxide (MEKP) (TAP Plastic) was added as catalyst (initiator) for all the three resins. A detailed study conducted on the resin cure kinetics can be found in Appendix B.

Experimental procedure is outlined in a flow chart (Figure 3.2). Hybrid poplar strand preforms pre-pressed to different densities, following the methodology described in chapter 2, were used for resin transfer molding experiments. Resin impregnation occurs as the resin transfers through the fiber preform. The pre-pressed preforms were placed in the mold cavity and vacuum pump was turned on for five minutes prior to resin injection to expel the trapped air inside the resin injection cylinder, mold, and the tubes. Resin was then injected into the mold with injection cylinder through the inlet port. Vacuum was applied at the outlet port to provide additional driving force for rein flow. This process was halted with locking pliers once resin in the injection cylinder finished injecting. During the injection period, the mold was positioned vertically so that the resin flow was from the inlet port at the bottom to the outlet port on the top (Figure 3.3); this allowed for the resin to gradually fill the preform. A video camera was used to record the resin flow. After the resin filled the cavity, both the outlet and inlet tubes were pinched with locking pliers and vacuum was turned off. The panel was left inside the mold to cure at room temperature till it reached its rigid state. Post-curing was then carried out in a forced air oven at 120°C for 4 hours (Caba, Guerrero, Eceiza, & Mondragon, 1996; Naffakh, Dumon, & Gerard, 2006; Rouison et al., 2004).

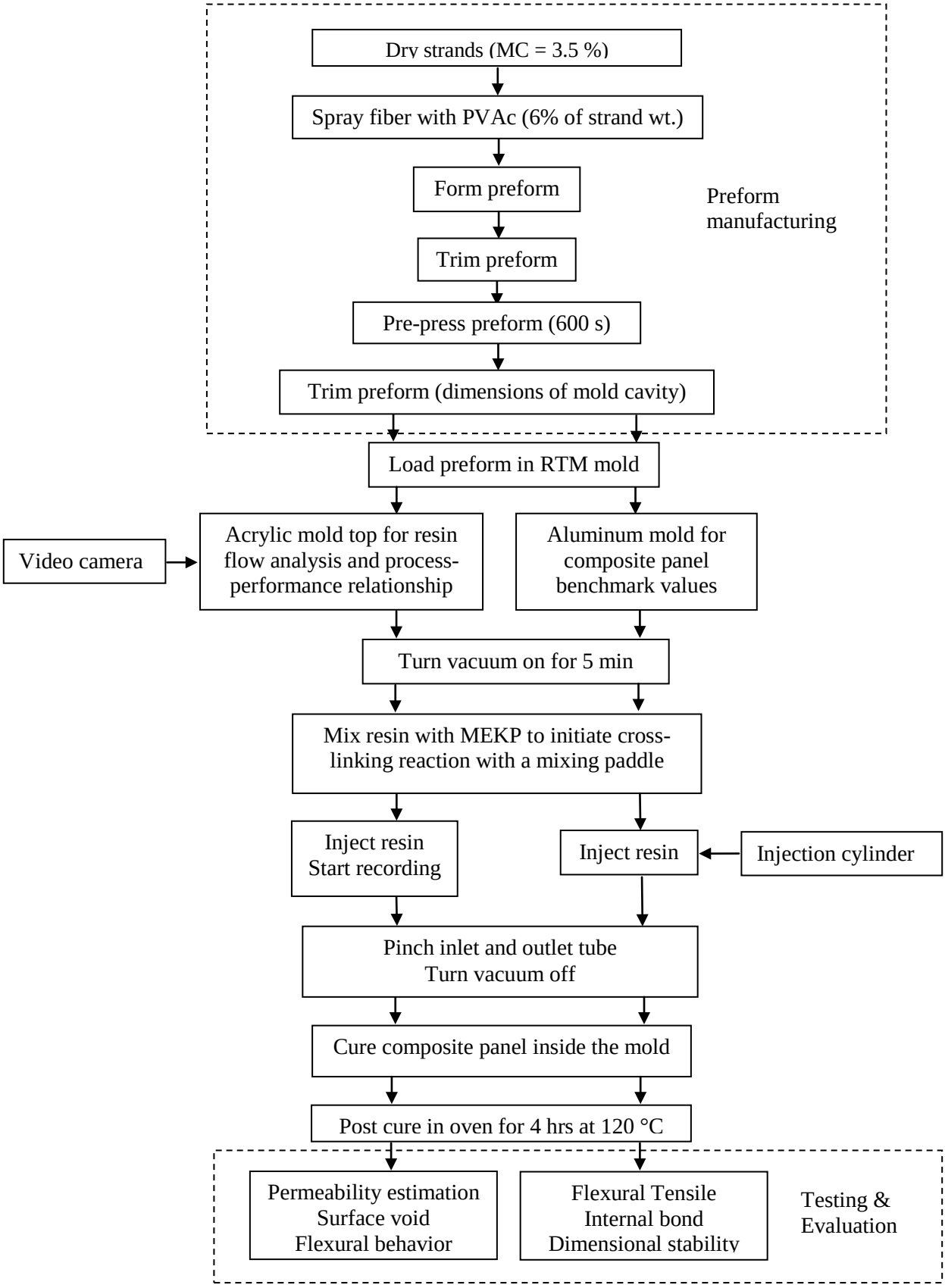

Figure 3.2 Experiential flow of resin transfer molding with both transparent and aluminum mold.

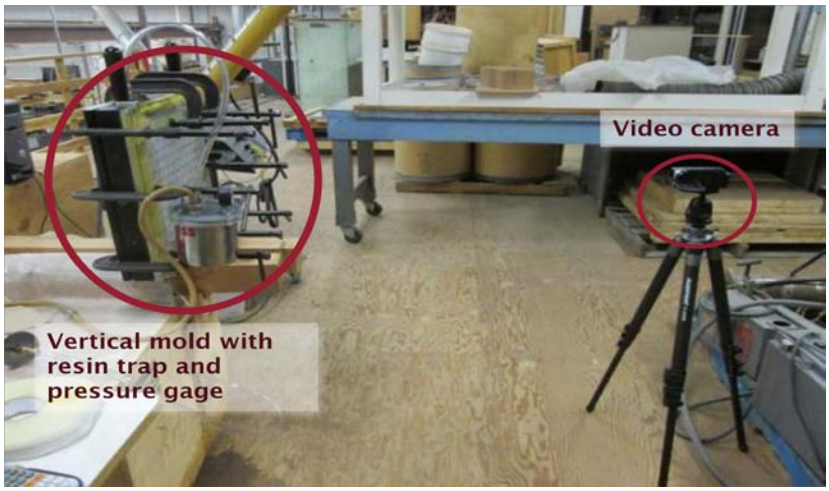

Figure 3.3 Experimental set up for resin flow analysis – video taping of the resin flow.

Snapshots of the resin flow video were generateed with Free Video to JPG Converter to extrat frames every 0.5 to 5 seconds based on the fill time. These snapshots were then analyzed with Photoshop to track the resin flow front with a red line and five points were evenly chosen along this line (Figure 3.4). The average distance from the inlet port to the five points was considered as the flow front position at an instanteneous time t (Figure 3.4). These data was further analyzed for permeability estimation.

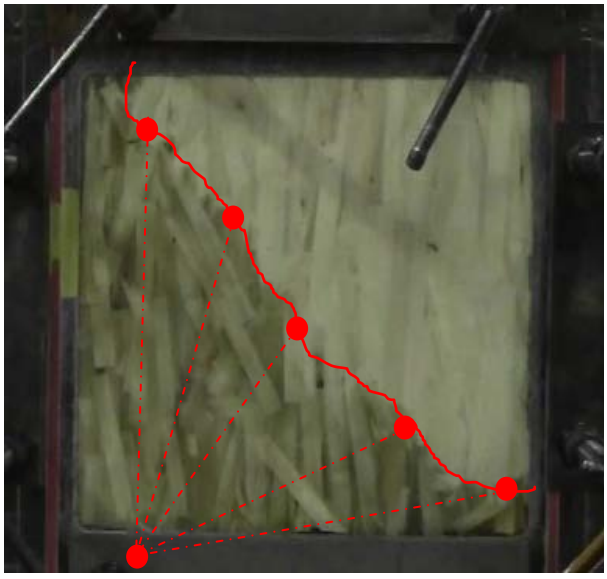

Figure 3.4 Flow front position determined with averaged distance of five points on the front.

3.3.2 Permeability Evaluation

3.3.2.1 Permeability Estimation Equations

Permeability describes the ease with which fluids move through a porous solid under the influence of a pressure gradient. According to Darcy's law, the permeability can be stated as in Equation 3.1.

$$k = \frac{\text{Flux}}{\text{Gradient}} = \frac{Q}{A\Delta P} = \frac{V}{tA\Delta P} \qquad \text{Equation 3.1}$$

Where,

k = permeability in m^3 (liquid)/m Pa s

Q = volumetric flow rate in cubic meter per second (m^3/s)

L = length in flow direction in meters (m)

V = volume of flow in cubic meter (m^3)

A = cross section area of the flow front in square meter (m^2)

ΔP = pressure gradient in Pascal per meter (Pa/m).

According to Siau (1995), permeability often used is the specific permeability, which is the product of permeability and the viscosity of the fluid. Since these quantities are inversely proportional, specific permeability should remain the same regardless of the fluid used.

$$K = k \times \mu \qquad \text{Equation 3.2}$$

where, K is the specific permeability in square meter (m^2), and μ is the fluid viscosity in Pa s (1 Pa s = 1000 cP).

Note that, permeability k varies with testing fluid. However, by taking testing fluid viscosity into consideration, specific permeability remains the same if the testing fluid dose not interact with the fiber preform, and additionally the fiber preform remains its geometric shape during fluid transferring.

Substituting Equation 3.2 into Equation 3.1, and dividing both the top and bottom by the area leads to

$$K = \frac{Q\mu}{A\Delta P} = \frac{q\mu}{\Delta P} \qquad \text{Equation 3.3}$$

where, q is the flux (discharge per unit area) with units of length per time (m/s).

Fluid velocity v is related to Darcy's flux (q) by the flow medium (the fiber preform) porosity (ϕ) shown below:

$$v = \frac{q}{\emptyset} \qquad \text{Equation 3.4}$$

where v is the fluid velocity with units of length per time (m/s).

By taking account only the porous medium that is available for fluid flow and substituting Equation 3.4 into Equation 3.3, gives the most commonly used Darcy's law shown below:

$$K = \frac{v\emptyset\mu}{\Delta P} \qquad \text{Equation 3.5}$$

Three approaches were applied to estimate permeability with the following assumptions:

- Porosity in the preform in assumed homogeneously distributed
- Permeability along the fiber direction is considered to be constant for a given preform
- Temperature and resin viscosity were assumed to be constant during resin injection process
- Resin is assumed to be a Newtonian fluid
- Incompressible fluid

The first approach is derived from Darcy's law when considering one dimensional simulation, where $\frac{\partial P}{\partial x} = \frac{P}{x}$ is assumed. Applying this relationship, permeability can be obtained by integrating both sides (see Equation 3.6 to Equation 3.9).

$$v = \frac{K}{\mu\emptyset}\Delta P \quad \rightarrow \quad \frac{dx}{dt} = \frac{K}{\mu\emptyset}\frac{\partial P}{\partial x} \qquad \text{Equation 3.6}$$

$$x \cdot dx = \frac{K}{\mu\emptyset} \cdot P \cdot dt \qquad \text{Equation 3.7}$$

$$\int_0^x x \cdot dx = \frac{K}{\mu\emptyset} \cdot P \int_0^t dt \qquad \text{Equation 3.8}$$

$$x_f{}^2 = \frac{2K_1}{\mu\emptyset} \cdot Pt \qquad \text{Equation 3.9}$$

where x_f is the flow front position in meters (m) (varies from 0 to the distance between inlet and outlet port), P is the pressure, K_1 is the permeability of the first approach, μ is viscosity, t is the time. The slope of the linear regression of x_f^2 verses t provides an estimate of permeability, K_1.

The second approach is the average permeability of every time period (t_i), shown below.

$$K_i = \frac{v(t_i)\mu\emptyset}{\frac{dP}{dx}} \qquad \text{Equation 3.10}$$

$$V_{t_i} = \frac{1}{2}\left(\frac{x_{i+1} - x_i}{t_{i+1} - t_i} + \frac{x_i - x_{i-1}}{t_i - t_{i-1}}\right) \qquad \text{Equation 3.11}$$

$$\frac{dP}{dx} = \frac{P}{x_f} \qquad K_2 = \frac{1}{t}\sum_{i=1}^{i=t} K_i \qquad \text{Equation 3.12}$$

where P is the flow front pressure in Pascal (Pa), t is the fill time when the mold is fully filled in second (s), x_i is the flow front position at time i in meters (m), and K_2 is the permeability estimated using approach two.

The third approach to estimate permeability is using Carman-Kozeny equation (Equation 3.13).

$$K_3 = \frac{r_f^2}{4K_z}\frac{\emptyset^3}{(1-\emptyset)^2} \qquad \text{Equation 3.13}$$

where K_3 stands for permeability approach three, r_f is the fiber radius, K_Z is the Kozeny constant along fiber direction, usually assumed to be between 0.4-0.7 (Demaria, Ruiz, & Trochu, 2007). Thickness was considered as the fiber diameter, which means r_f =1/2 the thickness of a wood strand.

Porosity was determined using the fiber volume fraction, V_f, which is the volume percentage of the fiber, defined in Equation 3.14. It is directly related to the preform permeability, which will in turn influence the resin flow rate, filling time, and flow front position. Porosity is the void space in preform represented as ϕ in Equation 3.15. Each preform density was used in Equation 3.9, Equation 3.12 and Equation 3.13 for permeability estimation.

$$V_f = \frac{v_p - \frac{m_p - m_f}{\rho_r}}{v_p} \times 100\% \qquad \text{Equation 3.14}$$

$$\emptyset = 1 - V_f \qquad \text{Equation 3.15}$$

where the subscript p, f and r represent panel, fiber and resin, respectively, and resin densities are given in Table 3.1.

Note that the resin is not the PVAc adhesive used in Chapter 2 but the thermosetting resins that wet and impregnate the fiber preform. And the porosity is not the same as the void volume described in Chapter 2 (which accounted for both micro- and macro-voids as it was based on cell wall density). Instead, the

porosity only includes the voids that can be filled with resin, which should be lower than preform void volume.

3.3.2.2 Influence of Processing Variables on Panel Quality

Four force components were always considered in the resin flow plane: injection pressure, vacuum, capillary pressure and gravitational pressure. Capillary force is defined as the energy per unit volume of a porous medium needed for replacing a gas by a liquid (Francucci & Vázquez, 2012) and is often negligible, and thus neglected in RTM for the ease of analysis. Gravitational pressure was considered as a constant for all the experiments for the same setup, therefore was ignored. On the other hand, injection pressure was the main driving force for the resin flow, and vacuum influences the compressibility of the preform. In this study, only injection and vacuum were taken into consideration.

Responses evaluated, to establish the influence of the processing variables on panel quality, were surface void content and flexure behavior of composite panels made using the acrylic mold top.

3.3.2.2.1 Panel Surface Void Evaluation

Voids formation during resin transfer is inevitable. Many studies have been conducted on the formation of voids and methods to reduce the voids (Barraza et al., 2004; Leclerc & Ruiz, 2008). In this study, surface voids on panels manufactured in Phase 1 were circled and quantified with Photoshop (Figure 3.5). The percentages of surface voids were calculated based on the panel surface area. Both the top and bottom surface voids were analyzed for each panel.

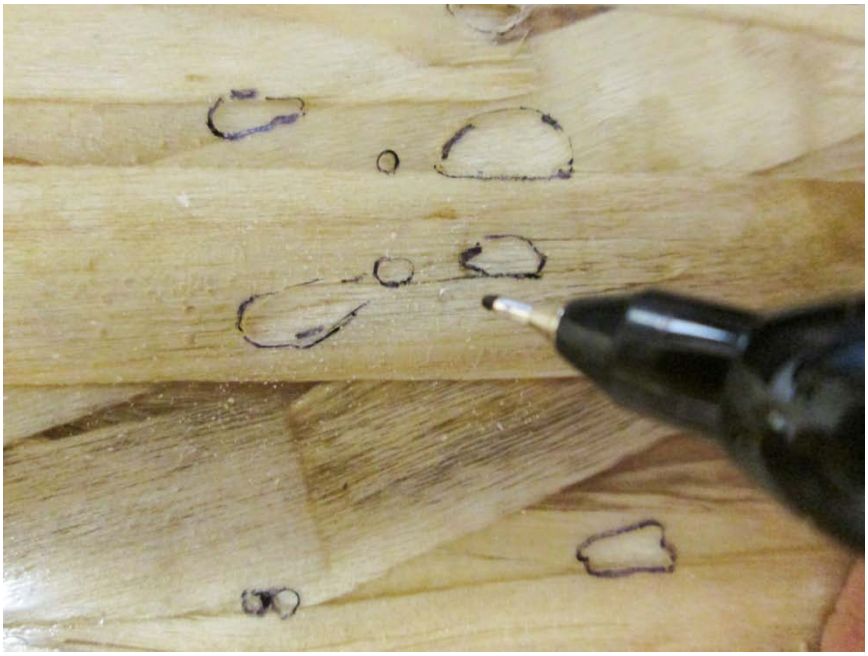

Figure 3.5 Circling the surface voids and ready to calculate using Photoshop.

3.3.2.2.2 Static Bending Properties of Composite Panels

Flexural properties including modulus of rupture (MOR) and apparent modulus of elasticity (MOE) were determined following ASTM D1037 of specimens prepared from panels made with transparent acrylic mold (will be referred to as PMMA panels). The nominal thickness for PMMA panels is ~ 6.35 mm and the span was set at 152.4 mm to minimize influence of shear strain on bending deflection (Bodig & Jayne, 1982). The length of the specimens was trimmed to 280 mm. The diameter of rounded support was 19 mm. Specimens were all loaded face-up with load rate adjusted to average thickness of each specimen.

$$N = \frac{zL^2}{6d} \qquad \text{Equation 3.16}$$

where z is the outer fiber strain rate of 0.005 in mm/mm/min, L is the span in millimeter (mm) and d is the thickness of specimen in millimeter (mm).

3.3.3 RTM of Composite Panels for Performance Evaluation

For establishing benchmark performance values, the transparent mold top was substituted by an aluminum top to manufacture composite panels. Moreover, a press was used to hold the mold halves in place instead of using C-clamps as illustrated in Figure 3.6. Based on the first part of the study (resin flow analysis), injection pressure, vacuum and preform density were kept constant during the manufacturing of the composite panels. Three resins were used (Table 3.1) and 5 panels were made for each resin.

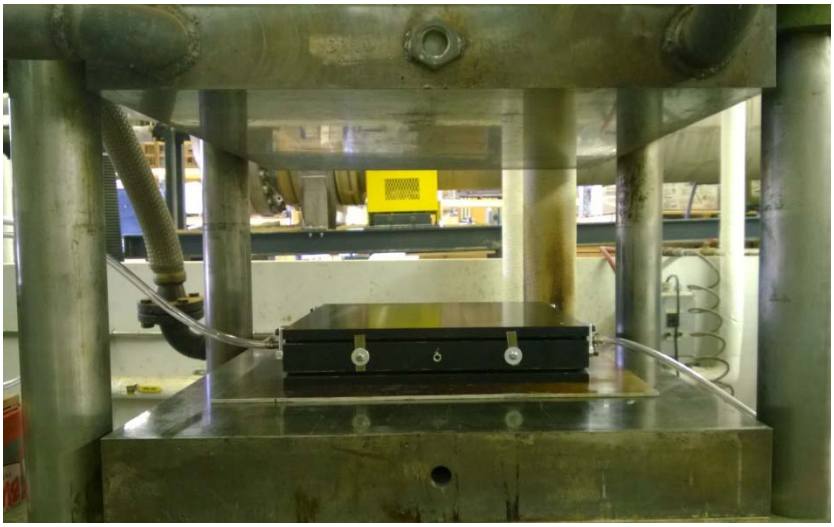

Figure 3.6 Mold was held in place using a hydraulic press during resin injection.

A press profile was developed to achieve the final thickness for ensuring a good resin impregnation and good fiber saturation as shown in Figure 3.7a. Gradual press closing to reach the final panel thickness is necessary to ensure proper impregnation and even distribution of resin in the preform. An improperly pressed and impregnated preform will lead to a poor quality panel as shown in Figure 3.7b. A typical pressure profile to reach final thickness is shown in Figure 3.8. Pressure was monitored as the mold was closed to the desired thickness of the preform/panel. The mold was first pressed to 80-mm, and vacuum was turned on, resin started to inject after five minutes of vacuum. Mold was checked to ensure that it was sealed which was confirmed by vacuum buildup. However, when the mold is fully closed, the thickness was 79-mm (depth of mold cavity was 79-mm at this point). Injecting resin as mold cavity was closed gradually to a final thickness of 79 mm allowed the resin to distribute evenly and impregnate into the

preform voids. Minute adjustments of the pressure profile were made depending on the resin type (to adjust for viscosity).

a) Panel #15 shows a good resin impregnation and good fiber saturation

b) Bad resin impregnation (trial experiment)

Figure 3.7 Good and bad resin impregnation examples.

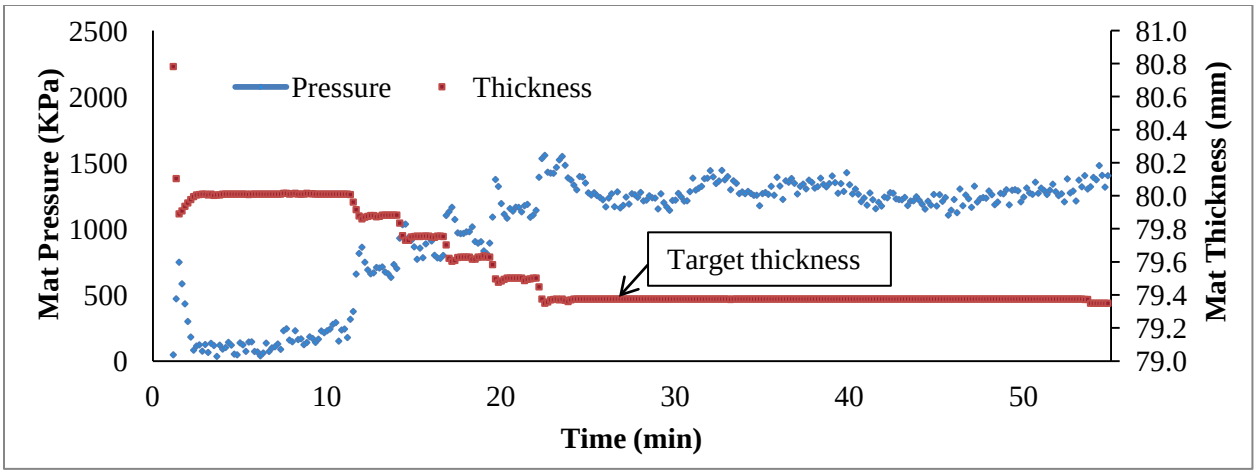

Figure 3.8 A typical pressure profile for fabricating testing panels.

Mechanical properties including modulus of elasticity (MOE) and modulus of rupture (MOR) in bending, tensile strength, tensile Young's modulus (E), and tension perpendicular to surface (internal bond) were evaluated according to ASTM D1037-12. Dimensional stability of the finished panels was evaluated by quantifying water absorption (WA) and thickness swell (TS) as per ASTM D1037-12.

3.3.3.1 Static Bending Properties

Flexural properties including modulus of rupture (MOR) and apparent modulus of elasticity (MOE) were determined following ASTM D1037 of specimens prepared from panels made with rigid aluminum mold (referred to as AL panels).

The nominal thickness for AL panels was ~ 3.175 mm and the span was 203 mm. The length of the specimens was trimmed to 241 mm. The diameter of rounded support was 12.7 mm. Specimens were all loaded face-up with load rate adjusted to average thickness of each specimen. A LE-03 laser extensometer was utilized with reflecting tape installed on specimens for deflection measurements during bending tests (Figure 3.9).

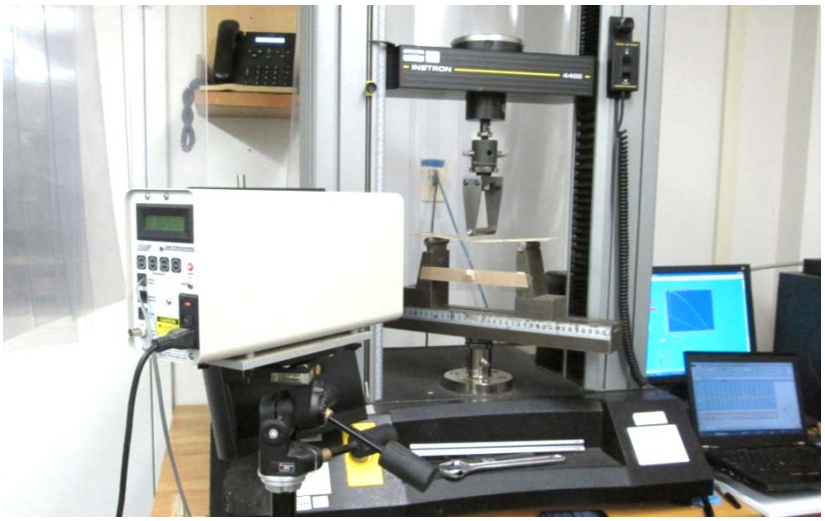

Figure 3.9 Static bending test to determine flexure properties. Specimen deflection was measured using a laser extensometer.

3.3.3.2 Tension Parallel to Preferred Orientation of the Strands (machine direction)

Tensile strength and modulus in the direction of the panel that is parallel to the long axis of the strands were determined using dog-bone shaped specimens with ~20-mm reduced mid-section where strain was measured using an extensometer (Figure 3.10). Wedge action grips with 50-mm square jaw faces were used to provide tightening force and prevent slipping. Speed of testing was 4 mm/minute. A 51-mm gage length extensometer over the reduced section of the specimens was used to measure longitudinal strain.

Figure 3.10 Tension test specimen with reduced section.

3.3.3.3 Internal Bond (Tension Perpendicular to Surface of Panels)

Internal bond specimens were cut from RTM fabricated panels with aluminum mold and tested as per ASTM D1037-12. Specimens were 2 by 50-mm cross section and load blocks were glued to the surfaces to apply load in the thickness direction. The two surfaces of each specimen were sanded for better adhesion with the metal blocks. Internal bond test is a good quality control test to ensure adequate bonding between strands. It is an effective indicator of good penetration of resin through preform thickness.

3.3.3.4 Water Absorption and Thickness Swell

Dimensional stability was evaluated by determining water absorption and thickness swell following the ASTM standard D1037-12. One specimen was cut from each panel and was trimmed to 152 by 152 mm with all four edges smoothly and squarely trimmed. Prior to testing, specimens were conditioned in a room maintained at a relative humidity of 50 ± 5% and a temperature of 21 ± 3 °C. Method A with horizontal submersion in water was used (Figure 3.11). Moisture content was determined afterwards following method A in ASTM standard D4442.

Figure 3.11 Testing specimens with horizontal submersion

3.3.3.5 Vertical Density Profile

Two 50 × 50 mm specimens (one near edge and on near center) were cut from each of the finished panel and an X-ray densitometry (QMS Model QDP-01X) was used to measure the vertical density profile (through thickness density variation). The resolution of the testing was 0.054 mm.

3.3.4 Rule of Mixtures to Predict Composite Panel's Young's Modulus in Tension

Molded composite panel property highly depends on both fiber and resin matrix properties. Wood strands, used for fabricating preforms and panels, were tested in tension to evaluate their strength and stiffness. Wood is generally assumed to be an orthotropic material, where modulus of elasticity varies with material axes. Strands were tested in tension parallel to grain based on the method proposed by Yadama et al. (2006). A 12-mm gage length axial extensometer (Epsilon Model 3442) was installed in the mid section of each strand (Figure 3.12). The specimens were loaded at a uniform crosshead speed of 0.4-mm/minute until failure.

Young's modulus of the composite panel can be predicted according to the rule of mixtures (Equation 3.17).

$$E_c = V_f E_f + (1 - V_f) E_r$$ Equation 3.17

where, $c, f \ and \ r$ stand for composite, fiber and resin, respectively, V_f is the fiber volume fraction, and E is the Young's modulus parallel to the longitudinal direction in case of the strands and the composite.

Figure 3.12 Testing of a wood strand in tension parallel to the longitudinal axis (general grain direction). A 12-mm gage length extensometer was installed at mid length to record longitudinal strain.

To determine average density of wood strands, several wood strands were weighted and then covered with known weight paraffin wax. They were full submerged into the distilled water in a graduated cylinder. Wood strand volume was measured with Archimedes' principle by subtracting the volume of the paraffin wax. Wood strand density was then calculated using the wood strand volume.

3.4 Results and Discussion

Resin flow data collected in section 3.3.1.1 was used to determine permeability using three different approaches described in section 3.3.2.1. Surface void and flexural properties of PMMA specimens (section 3.3.2.2) were statistically analyzed with response surface method (RSM) to evaluate the influence of processing parameters including injection pressure, vacuum, resin viscosity, and preform density. The

three permeability estimation approaches were also compared to determine the best approach for wood strands preform permeability estimation. Linear models were used for these evaluations. Mechanical, water absorption and thickness swelling properties of AL specimens from composite panels (section 3.3.3) were determined to establish benchmark values. Statistical analysis was conducted to compare the properties of the RTM fabricated panels using the three resins.

3.4.1 Specific Permeability

Flow front position at an instantaneous time was determined in section 3.3.1.1. The resin flow front position over time for run #1 in Table 3.3 is shown in Figure 3.13. Flow front exhibits linear relationship with time under constant injection pressure and vacuum. Based on this plot, the slope of the fitted linear regression of flow front position x_f^2 (m^2) vs. time t (s) can be determined. Substituting the slope into Equation 3.9, specific permeability with approach one (K_1) can be calculated. In the following discussion, permeability was used for specific permeability described in the permeability estimation equations.

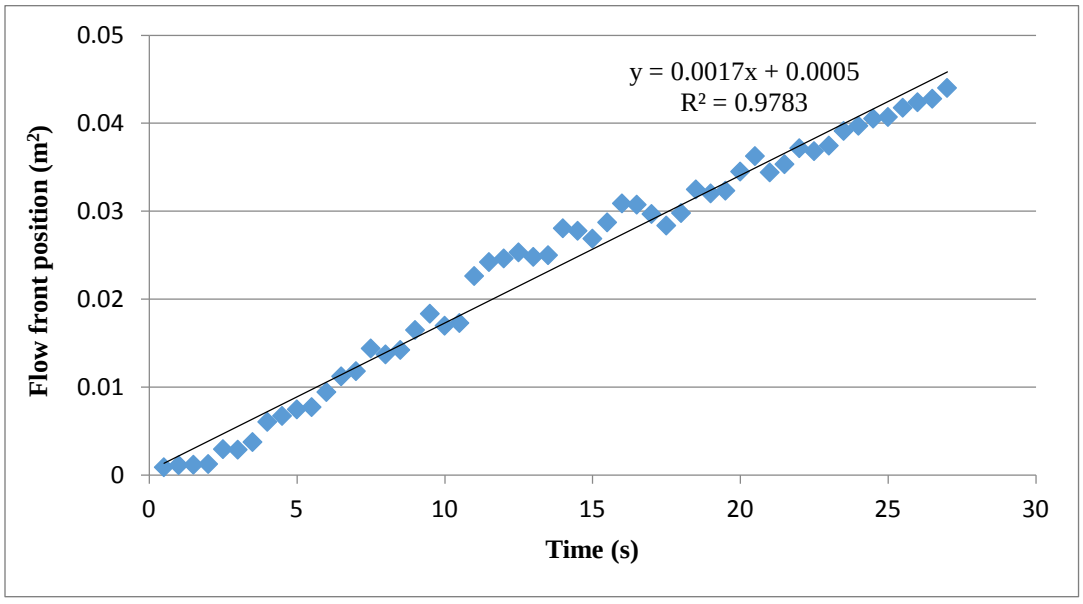

Figure 3.13 A typical plot of flow front position (m^2) over time (s).

ANOVA for permeability approach one (K_1) (Table 3.4) indicated that a linear model to be significant (p-value 0.0042); therefore it was used for analyzing the influence of each parameter. Moreover, influences of resin viscosity and preform density were statistically significant. The reduced linear model with their coefficients is shown in Equation 3.18. Its corresponding plot is shown in Figure 3.14a. Similar analysis for permeability approach two (K_2) and approach three (K_3) can be found in Appendix C. Their corresponding response surface graphs are shown in Figure 3.14 b and c.

As preform density increases, permeability (K_1) of the preforms decreases as expected (Figure 3.14). Preform density is related to fiber volume fraction, and a low fiber volume fraction corresponds to a larger permeability, which has already been established by other authors (Buntain & Bickerton, 2003). As expected, permeability for any given preform density increases as viscosity of the resin decreases. This trend is similar to what was reported for other reinforcing fiber preforms (Ma & Shishoo, 1999) where permeability is inversely proportional to the fluid viscosity. Influence of resin viscosity on permeability was statistically significant (p-value=0.0016), indicating a need to ensure that adequate resin penetration is ensured with higher viscosities by controlling other parameters, such as increasing void content. Though the injection pressure is not a statistically significant variable, results show a stronger correlation between injection pressure and permeability for lower density preforms. Many researchers (Amico & Lekakou, 2001; Lundström, Stenberg, Bergström, Partanen, & Birkeland, 2000) have studied the influence of injection pressure on the permeability and reported that permeability is independent of injection pressure. Influence of preform density on permeability using method one (K_1) is shown in Figure 3.14a and 3.14b. It can be seen that at low preform density (320 kg m^{-3}), permeability is directly proportional to the injection pressure, a trend that was also observed by Lekakou et al. (1998). As specific permeability is directly related to viscosity as shown in Equation 3.2, higher resin viscosity results in higher permeability; however, different resin types due to their chemistry and physical characteristics could interact differently with preform material and influence the resin flow. Resin C shows a strong interaction between the resin and the wood strands in the preform.

A combination of higher void content and injection pressure provides a greater driving force for resin to transfer and flow through the preform. Further analysis is required to arrive at conclusive evidence. At high preform density (640 kg m^{-3}), permeability using first and second methods (K_1 and K_2) shows an increasing trend with injection pressure; however, K_3 decreases with increased injection pressure. This could be because and permeability (K_3) is highly dependent upon the preform porosity and higher density preforms have fewer voids. Additionally, resin under high injection pressure may violate the Darcy's law and result in increasing of Reynolds number, when the mechanism violates assumptions of Darcy's law (Daniel, 2007). The general trend is higher injection pressure yields higher permeability, however this effect can be influenced by the preform density and resin viscosity. A suitable range of injection pressure therefore needs to be identified, depending on the preform density, to ensure a sufficient resin impregnation. When using lower density preforms, resin fill time can be significantly reduced with higher injection pressure as it has a greater impact on permeability.

Table 3.4 ANOVA for permeability approach one (K_1) with estimated coefficients.

Source	Sum of Squares	df	F-value	P-value	Coefficient
Model	27.70762	4	8.451136	0.0004*	4.2690
A-Injection pressure	2.95236	1	3.602012	0.0722	
B-vacuum	0.123313	1	0.150447	0.7022	
C-resin viscosity	10.85001	1	13.2375	0.0016*	4.8842E-3
D-preform density	10.62116	1	12.95829	0.0018*	-5.5396E-3
Residual	16.39284	20			
Lack of Fit	14.33743	17	1.230964	0.4955	
Pure Error	2.055409	3			

*Significant variables

$$K_1 = 4.2690 + 4.8842\text{E} - 3 \times A - 5.5396\text{E} - 3 \times D \qquad \text{Equation 3.18}$$

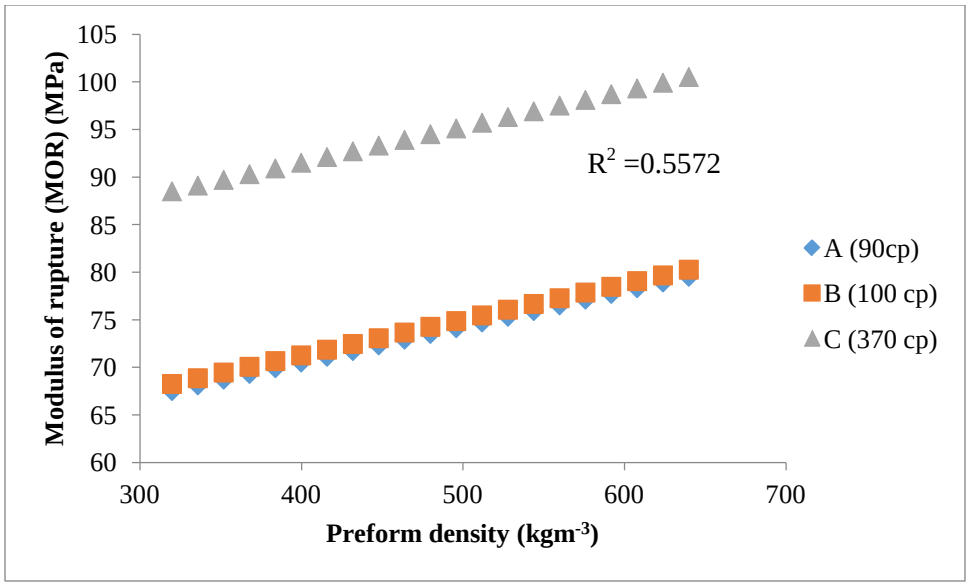
Modulus of rupture (MOR) (MPa)
105
100
95
90
85
80
75
70
65
60
300
400
500
600
700
Preform density (kgm-3)
R2 =0.5572
A (90cp)
B (100 cp)
C (370 cp)

a)

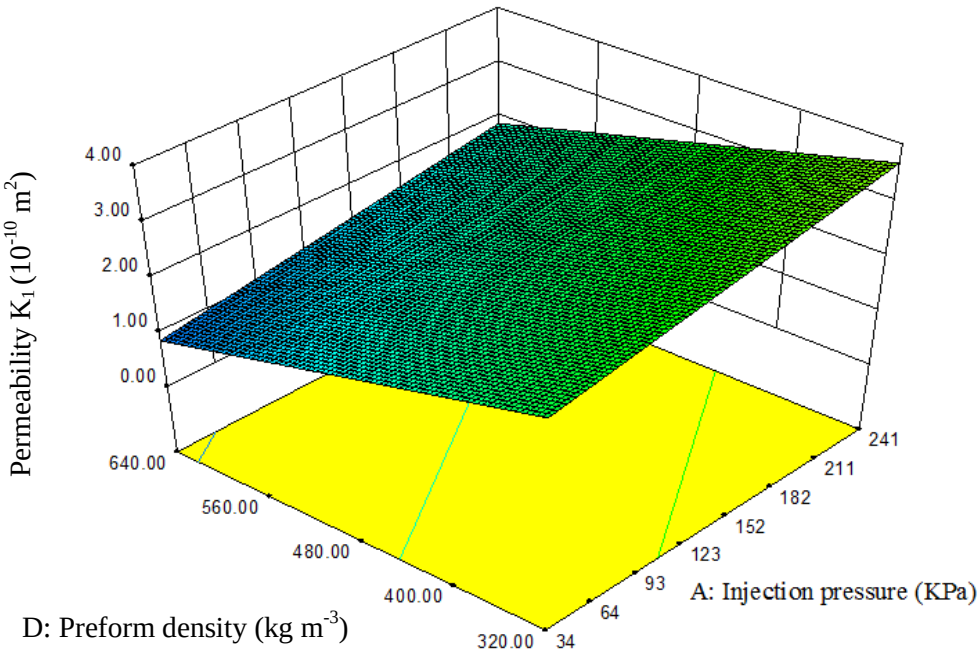
Permeability K1 (10-10 m2)
4.00
3.00
2.00
1.00
0.00
640.00
560.00
480.00
400.00
320.00
D: Preform density (kg m-3)
34
64
93
123
152
182
211
241
A: Injection pressure (KPa)

b)

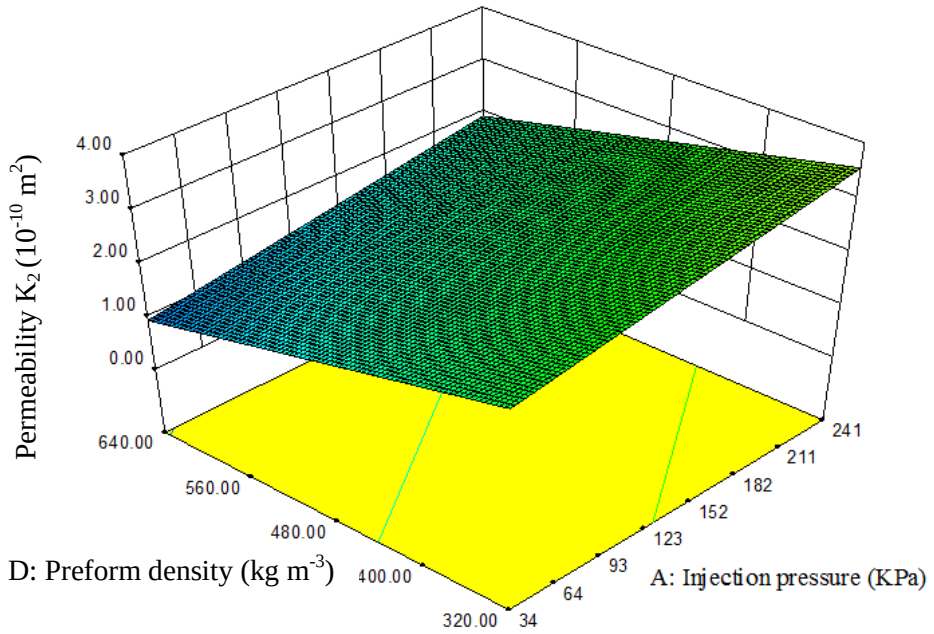

c)

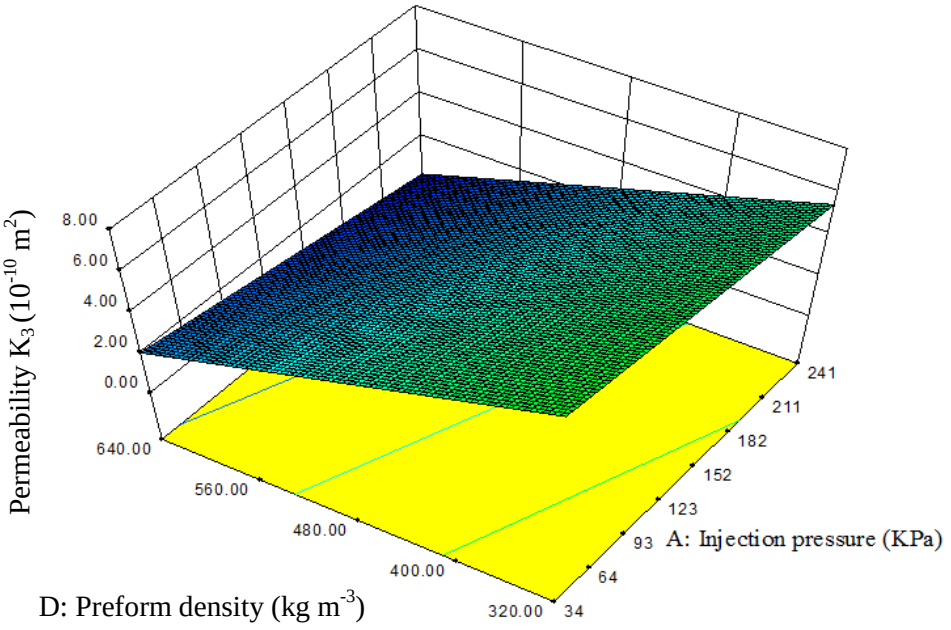

d)

Figure 3.14 Linear model of permeability (K_1) as a function of (a) preform density, (b) response surface of injection pressure and preform density using method one, (c) method two, and (d) method three.

Permeability for wood strand preform does not always remain constant (Demaria et al., 2007), and higher porosity tends to have higher K_Z. Note that when using 0.4-0.7 as K_Z, the permeability did not properly fit permeability K_1 and K_2. As the K_Z varies, permeability estimated using Carman-Kozeny equation alters (Figure 3.15). The estimated permeability at porosity 0.60 and 0.75 with the first and second method is approximately 1.25 x 10^{-10} m^2 (shown in gray dash lines). Estimated permeability with the third method decreases as Kozeny constant increases. Hence, as suggested by Rodriguez et al. (2004), K_Z in this study was adjusted to 2. Comparisons between permeability and fiber porosity are shown in Figure 3.16. Larger porosity fiber reinforcements clearly correspond to higher permeability, with an exponential increase with increase in porosity. The results with hybrid poplar wood strands as reinforcement follow the same trend, an exponentially increasing permeability with increase in porosity, especially above 0.6 (Figure 3.15b).

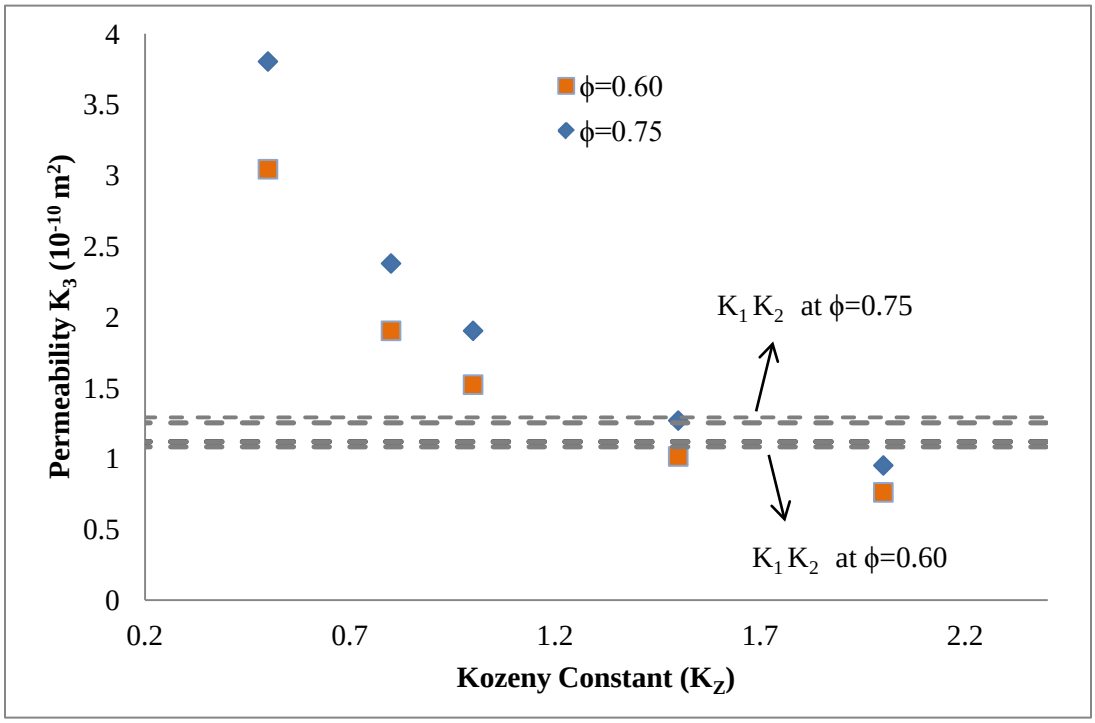

Figure 3.15 Carman-Kozeny equation to the relationship of Kozeny constant (K_Z).

The carbon fiber warp mat with 50% fiber volume fraction has permeability of 5.39x10^{-10} m^2 (± 12%), and permeability for E-glass fiber warp mat with 50% fiber volume fraction is 4.45 (± 10%) 10^{-10} m^2 both

measured with polyethylene and water polyol (26-27 cP) (Arbter et al., 2011). Permeability of wood in the longitudinal direction was studied by Siau (Siau, 1995). Red oak has the highest permeability with 2 $x10^{-10}$ m^2 due to the large early wood vessels. Permeability for wood strand preform in this study could be approximated to 2 $x10^{-10}$ m^2. Umer et al. (2007) measured permeability for pine wood fiber preform which ranged from 0.005-0.4$x10^{-10}$ m^2 and 0.05-0.6$x10^{-10}$ m^2 for fiber volume fraction varying from 0.4-0.2 when measured with glucose syrup and mineral oil, respectively. The mineral oil, with viscosity 74-104 cP, is a non-polar fluid and believed to better mimic a current synthetic thermoset resin.

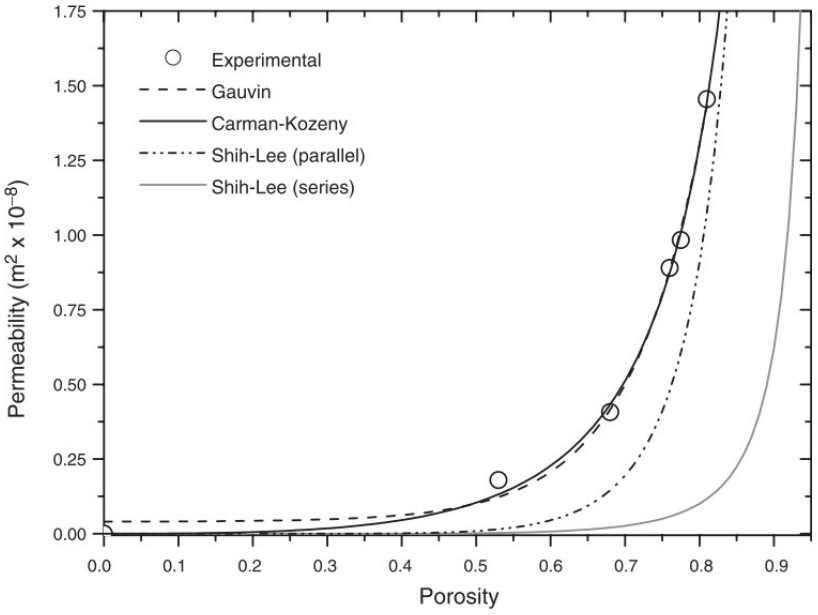

a)

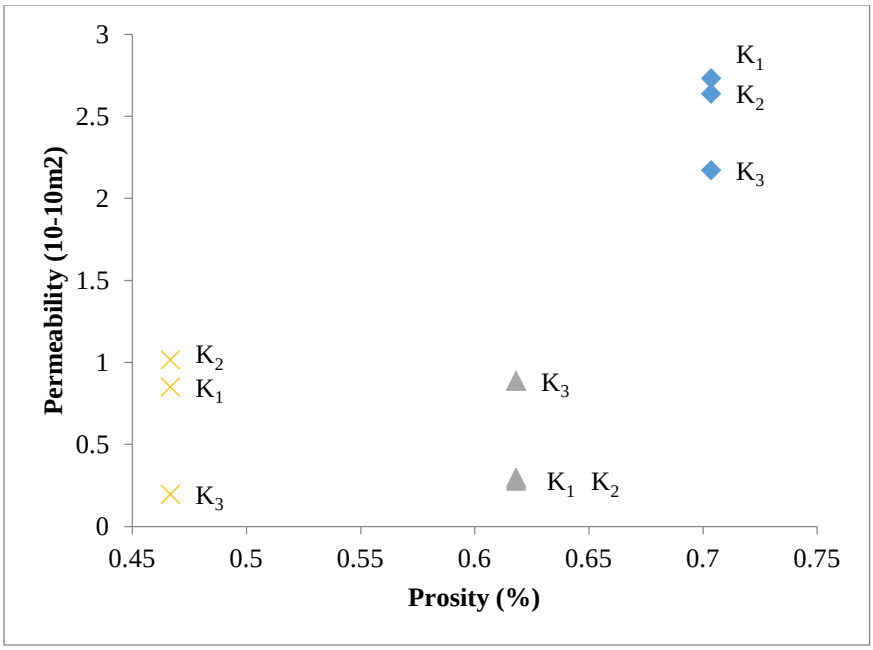

b)

Figure 3.16 Permeability and porosity relationships a) by Rodriguez et al. (2004)**;** b) experimental data measured in this study for wood strands preform.

Permeability values determined using the three methods were also statistically analyzed using ANOVA procedure (Table 3.5). There is not statistical difference in permeability computed using the three approaches (Table 3.5). Permeability approach one and two establish very similar results in this study. When experimental conditions meet the assumptions for using Darcy's law, these approaches can be very accurate. Moreover, when preform is uniformly distributed, pores are homogeneous, and the fiber does not interact with the resin (not a strong attraction to the fluid) then the Carman - Kozeny equation can be applied successfully (Demaria et al., 2007; Rodriguez et al., 2004). In this case, approach one and two are recommended for wood strands preform permeability estimation.

Table 3.5 ANOVA table for permeability estimations.

Source	Df	SumSq	MeanSq	F-value	P-value
Permeability	2	27.4	13.701	1.891	0.158
Residuals	72	521.7	7.245		

3.4.2 Influence of Processing Variables on Panel Quality

3.4.2.1 Panel Surface Void Evaluation

Vacuum played a significant role in determining the extent of surface voids formed (Table 3.6). Vacuum seems to play a vital role in expelling the air from the mold, compressing the preform, and assisting resin to freely flow on the surfaces. Higher vacuum probably generates lower surface voids (Figure 3.17) because the suction of vacuum removes air from the composite material. As the resin transferred against gravity and with vacuum port being on the top, it could have been easier for the air bubbles to travel upwards and merge as they are exiting through the outlet tube. Similar behavior has also been corroborated by other researchers (Hayward & Harris, 1990). They attributed the improvement in fiber wetting to the vacuum only, not to the resin pressure. Resin pressure corresponds to both injection pressure and vacuum.

Table 3.6 ANOVA for surface voids.

Source	Sum of Squares	df	F Value	P-value
Model	34.8888	4	1.29	0.3077
A: Injection pressure	1.09	1	1.45	0.2422
B: Vacuum	2.52	1	3.35	0.0820
C: Resin viscosity	0.0.021	1	0.029	0.8676
D: Preform density	7.107E-4	1	9.473E-4	0.9758
Residual	98.15	20		
Lack of Fit	8.93	17	0.26	0.9716
Pure Error	6.07	3		

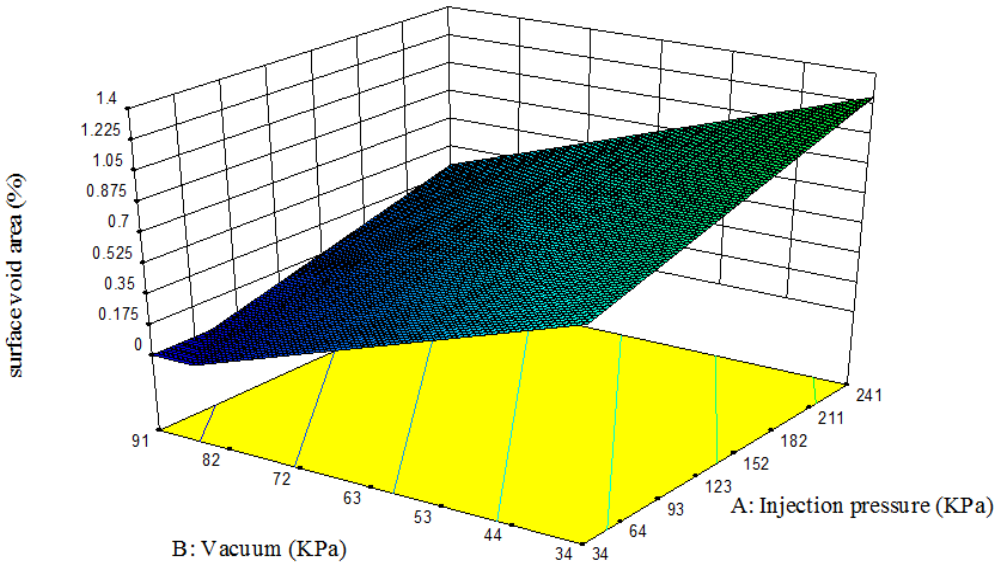

Figure 3.17 Surface voids as a function of injection pressure and vacuum.

3.4.2.2 Influence of Processing Factors on Static Bending Properties of PMMA Panels

Influence of processing variables on static bending behavior of panels manufactured using acrylic top (PMMA panels) was analyzed statistically (ANOVA). In case of MOE (Table 3.7), a linear model was suggested and found to be significant with a p-value < 0.0001. Preform density is the only significant variable, which is expected since a wood composite panel's mechanical properties are highly correlated with panel density. The estimated regression model with their coefficients is shown in Equation 3.19.

Increasing fiber volume fraction and, perhaps preform densification, resulted in increasing MOE with increasing preform density (Figure 3.18). Considering relationship between composite modulus and modulus of its constituents and their proportions (rule of mixtures), it is expected that composite modulus will be directly related to the perform density as it increases the fiber volume. Analysis also indicates that vacuum does play an important role (p-value = 0.0562), which could be justified by the fact that it tends to bring the preform together, thus reducing the void content and increasing its density.

Table 3.7 ANOVA for MOE with estimated coefficients.

Source	Sum of Squares	df	F-value	P-value	Coefficient
Model	14.09	4	11.3995	< 0.0001*	4.2887
A: Injection pressure	0.02	1	0.0724	0.7907	
B: Vacuum	1.27	1	4.1080	0.0562	0.0100
C: Resin viscosity	0.09	1	0.2831	0.6005	
D: Preform density	12.12	1	39.2255	< 0.0001*	5.2322
Residual	6.18	20			
Lack of Fit	3.95	17	0.3137	0.9496	
Pure Error	2.22	3			

*Significant variables

$$MOE = 4.2887 + 0.0100 \times \mathrm{B} + 5.2322 \times D$$ Equation 3.19

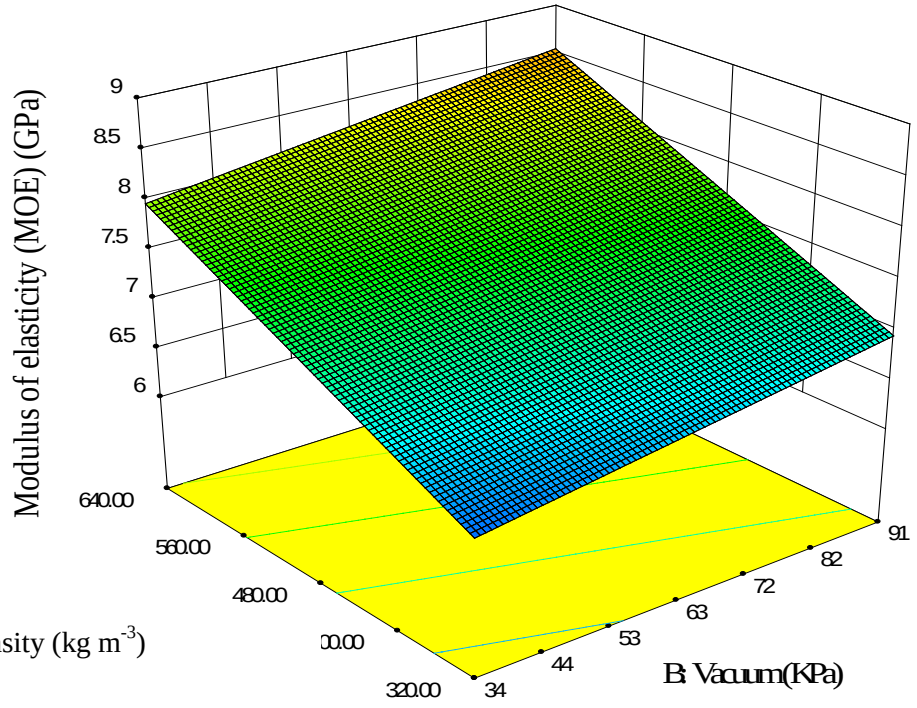

Figure 3.18 Linear model of MOE as a function of preform density.

Results of ANOVA for MOR with estimated coefficients are shown in Table 3.8. Once again, a linear model was suggested and found to be significant with a p-value = 0.0041. Resin viscosity and preform density play a significant role in determining MOR of the resulting composite panel. The estimated regression with their coefficients is shown in Equation 3.20. Corresponding plot is shown in Figure 3.19. Higher fiber volume fraction with increasing density and better bonding between the strands achieved with use of higher viscosity resin can explain the reason for an increasing MOR. Better bonding among the strands allows for effective transfer of stress between fiber and matrix. However, increase in MOR was not significant when viscosity was increased from 90 to 100 cP, even though strength of 100 cP resin is significantly greater than 90 cP (Table 3.1). These results indicate that resin with higher viscosity (370 cP) tends to wet the fiber better, considering that both 100 cP and 370 cP viscosity resins have similar strength values (Table 3.1). Lower viscosity resin perhaps does not wet the fiber as well and tends to flow through the preform too quickly. The increasing trend in permeability with increased viscosity (Figure 3.14a) also indicates that better fiber wetting is achieved with resins with higher viscosity. Fisher's LSD (least significant difference) pairwise comparisons were then evaluated for resin pairs in MOR (Table 3.9), and resin A (110 MPa) has significantly lower MOR than resins B (152 MPa) and C (152 MPa) (Table 3.1) Statistical analysis also shows that vacuum plays an important role (p-value = 0.0593) in providing suction force to remove air in the mold, compressing the preform, improving the bond between strands, and yielding a higher strength value.

Table 3.8 ANOVA for MOR with estimated coefficients.

Source	Sum of Squares	df	F-value	P-value	Coefficient
Model	3649.05	4	5.4024	0.0041*	48.74
A: Injection pressure	66.29	1	0.3925	0.5381	
B: Vacuum	675.33	1	3.9993	0.0593	
C: Resin viscosity	1687.04	1	9.9906	0.0049*	0.075
D: Preform density	763.08	1	4.5190	0.0462*	0.038
Residual	3377.27	20			
Lack of Fit	2850.81	17	0.9556	0.6025	
Pure Error	526.46	3			

*Significant variables

$$MOR = 48.74 + 0.075 \times C + 0.038 \times D$$ Equation 3.20

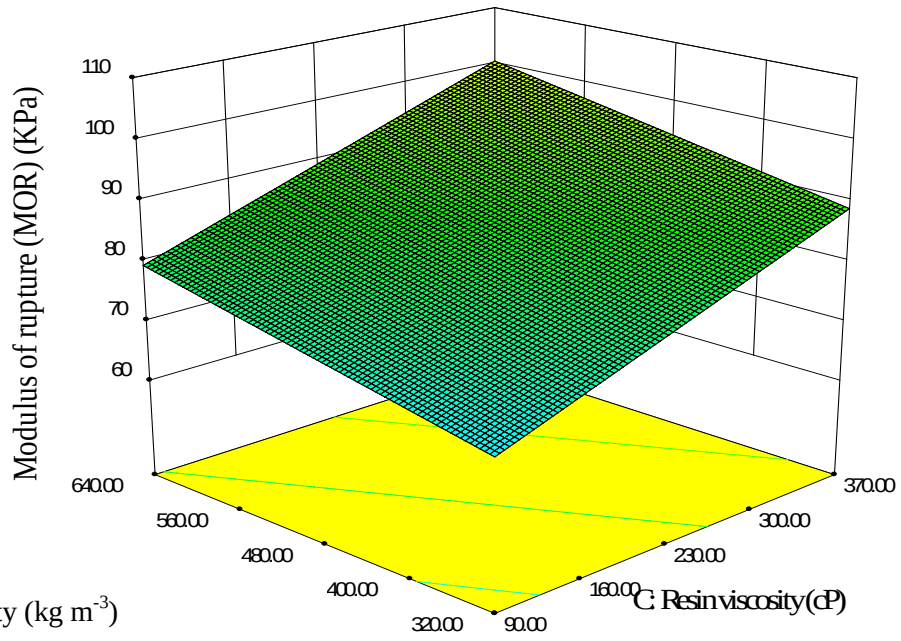

Figure 3.19 Linear model of modulus of rupture (MOR) as a function of preform density.

Table 3.9 Fisher's LSD test of resin pairs for MOR of PMMA panels.

Resin	Mean	Group[1]
A	63.5	a
B	85.0	b
C	93.6	b

3.4.3 Determination of Benchmark Performance of RTM Composite Panels

Since there is no published information regarding physical or mechanical properties of wood strand composite panels manufactured using RTM technology, one of the objectives of this study is to establish benchmark values for important composite properties. A summary of panel properties evaluated in this study along with published average properties of typical wood composite panels is shown in Table 3.10. In general, modulus of elasticity and strength values of RTM produced wood strand composite panels in tension and bending were greater than published values of typical wood-based composite panels manufactured currently. Although glass fiber panels were reported to have higher strength and stiffness than the ones produced in this study, when comparing specific strength values, panels produced in this study yield far better ratios. Performance of RTM produced wood strand panels in this study is superior to typical wood-based composites reported in other research studies, including water sorption performance and internal bond strength, an indicator of bond quality between strands. Hybrid poplar wood strand panels made with RTM compared to hybrid poplar OSB panels yielded significantly lower average water absorption (8.37% vs. 67%) and thickness swell (5.70% vs. 26.05%) values. Average IB strength also shows great advantage over hybrid poplar OSB (1.7 MPa vs. 0.7 MPa). For the RTM produced wood strand panels in this study, average panel density was 1116 kg m^{-3} with coefficient of variation (COV %) of 4.06 % considering all the panels across the three resin types. Therefore, panel density was not taken into consideration as a covariate in further statistical analysis. The variations of panel densities averaged across each resin are shown in Table 3.10.

Table 3.10 Selected property of wood strand composite panel and some typical materials in literature.

Material	Ave. Density	Static bending					Tension parallel to strand orientation		IB strength	WA	TS
		MOR	MOE	Specific strength	Specific stiffness	S	Tensile Strength	Tensile modulus		Wt.	
	kg m^{-3}	MPa	GPa	$KNmg^{-1}$	$MNmg^{-1}$	%	MPa	GPa	MPa	(%)	
Hybrid wood strand/ polyester	1105 (5.86)	83.56 (4.32)[a]	9.35 (3.60)	75.7 (4.28)	8.49 (9.32)	5.88 (67.54)	47.57 (26.35)	8.96 (10.53)	1.750 (26.41)	4.64 (38.04)	3.36 (86.56)
										11.13 (42.69)	7.26 (79.87)
Hybrid wood strand/vinyl ester	1114 (0.84)	108.29 (11.61)	10.61 (8.29)	97.2 (11.60)	9.53 (8.37)	2.87 (4.89)	75.67 (18.55)	10.10 (13.83)	1.795 (19.04)	3.7 (14.02)	1.77 (99.19)
										7.37 (0.10)	4.10 (0.88)
Hybrid wood strand/epoxy vinyl ester	1128 (5.36)	101.33 (23.07)	10.81 (8.83)	89.3 (19.20)	9.58 (6.11)	2.6 (9.18)	77.13 (19.60)	10.32 (10.40)	1.686 (10.36)	3.59 (10.21)	5.75 (87.59)
										6.63 (0.28)	1.93 (0.82)
Hybrid poplar solid wood[c]	360	32	7.1	88.9	19.72						
40% wood fiber/PP[d]	1030	47.9	3.25	46.5	3.16		28.2	4.20			
Sisal/vinyl ester[e]		72.7					31.8				
20 vol% hemp fiber/ polyester[f]	1230	54	5.02	43.9	4.08		32.9	1.421			
35 vol% hemp fiber/ polyester[f]	1230	112.9	6.38	91.8	5.19		60.2	1.736			
20 vol% glass fiber/ polyester[f]		175.9	7.74				85	1.719			
Aspen OSB[d]	650	32.2	6.28	49.5	9.66				0.43		12[h]

Note: MOR= modulus of rupture, MOE= modulus of elasticity, S = bending strain at break of, WA= water absorption, TS= thickness swelling.

[a] Values in parenthesis are coefficient of variation (COV %) of the averaged data.
[b] Data in bold represent the strength/density or stiffness/density ratio (MPa/kg m^{-3} or GPa/ kg m^{-3}).
[c] Data source: J. Balatinecz et al. Achievements in the utilization of poplar wood - guideposts for the future. Forestry Chronicle, 77 (2001) 265-269.
[d] Data source: wood handbook, Forest Products Laboratory, 2010.
[e] Data source: Y. Li. Processing of Sisal Fiber Reinforced Composites by Resin Transfer Molding. Materials and Manufacturing Process, 21: 181-190, 2006.
[f] Data source: D. Rouison et al. Resin transfer molding of hemp fiber composites: optimization of the process and mechanical properties of the materials. Composite Science and Technology, 66 (2006) 895-906.
[g]Data source: Q. Wu et al. Thickness swelling and its relationship to internal bond strength loss of commercial oriented strandboard. Forest products journal. 2007.
[h] Dara source: European Panel Federation. Results are for OSB/4-heavy-duty load-bearing boards for use in humid conditions.

3.4.3.1 Vertical Density Profile of Composite Panels

Vertical density profiles (VDP) show a constant density across the thickness of panels indicating a uniform consolidation and distribution of voids through panel thickness. This is a significant improvement over strand-based panels that are consolidated in a hot press where it is possible to find low-density cores even in relatively thin panels. Typical density profiles for each resin are presented in Figure 3.20. All panels had similar density of approximately 1200 kg m^{-3}. Density of panels with resin A (lower viscosity) is slightly lower and less homogeneous, whereas resin C (highest viscosity) yielded panels with slightly higher density. However, these results confirm that hybrid poplar wood strands composites manufactured with RTM process were on the average homogeneous across the thickness with minimum variation.

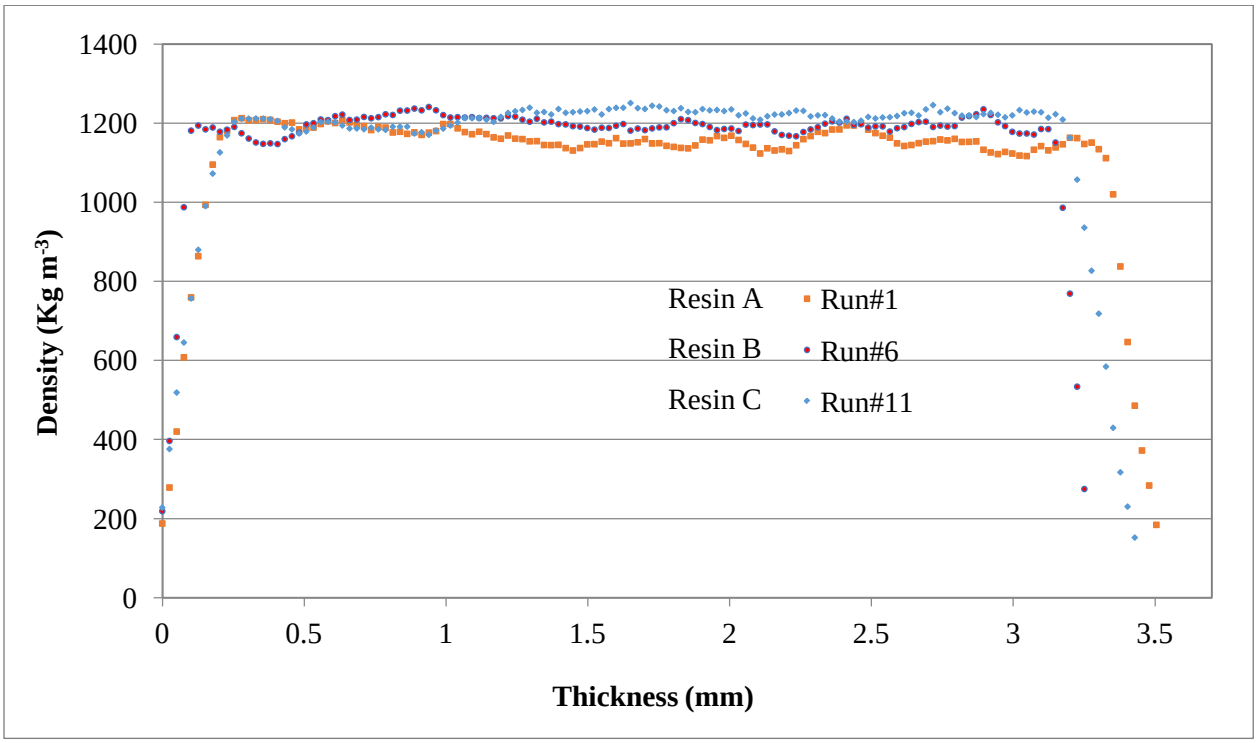

Figure 3.20 Vertical density profile (VDP) of panels produced with resin types A (Run #1), B (Run #6), and C (Run #11).

3.4.3.2 Static Bending Properties Parallel to Preferred Strand Orientation (machine direction)

Static bending results of specimens prepared from wood strand panels manufactured using the RTM process with aluminum mold (AL panels) were statistical analyzed (Table 3.11). Resin, although was shown to significantly influence MOE, did not play a critical role in determining either MOE or MOR. Fisher's LSD was conducted for resin pairwise comparisons (Table 3.12) of MOE, and no statistical difference was revealed among the three resins. Panels made with resins B and C always performed better in flexure than resin A (Figure 3.22), which is reflected in greater strength values for resins B and C compared to resin A (Table 3.1).

Table 3.11 ANOVA table of MOR and MOE of AL panel with resin.

	Source	Df	SumSq	MeanSq	F value	Pr(>F)
MOR	Resin	2	1412	705.9	2.718	0.1100
	Residuals	1	2858	259.8		
MOE	Resin	2	5.396	2.6981	4.215	0.0438*
	Residuals	1	7.041	0.6401		

*significant variable or interaction

Table 3.12 Fisher's LSD test of MOE of AL panels.

Resin	Mean	Group[1]
A	9.35	a
B	10.61	a
C	10.81	a

[1] Means with the same letter are not significantly different.

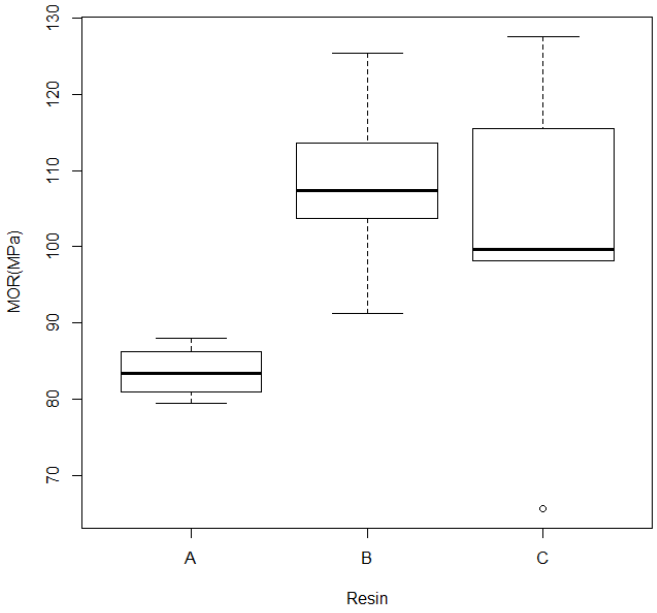

Figure 3.21 Influence of resin type on RTM wood strand panels with AL mold on MOR.

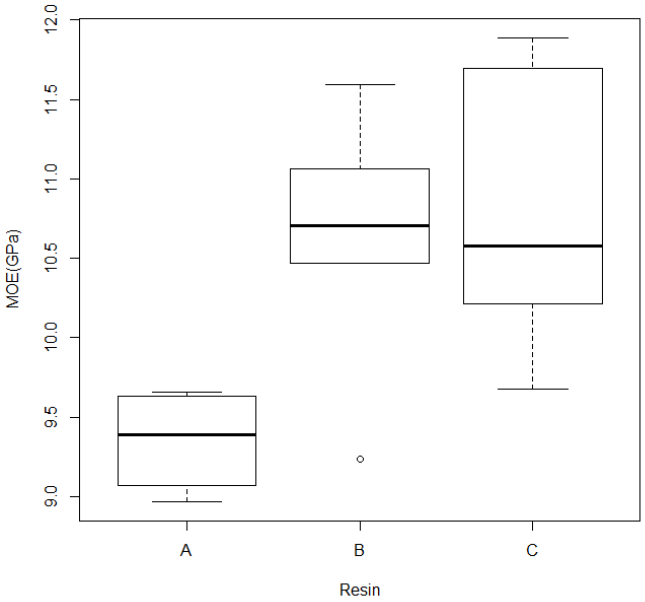

Figure 3.22 Influence of resin type on RTM wood strand panels with AL mold on MOE.

Stress-strain plots of different runs (varying resin type) are shown in Figure 3.23. Panels made with resin A (Run #1 and Run #2) exhibited lower MOE and higher strain at break, but panels made with resin B (Run #6 and Run #7) and resin C (Run #11 and Run #12) are stiffer and yielded lower strain at break compared to panels using resin A. Resin A seems to yield panels that are tougher than those manufactured using resins B or C.

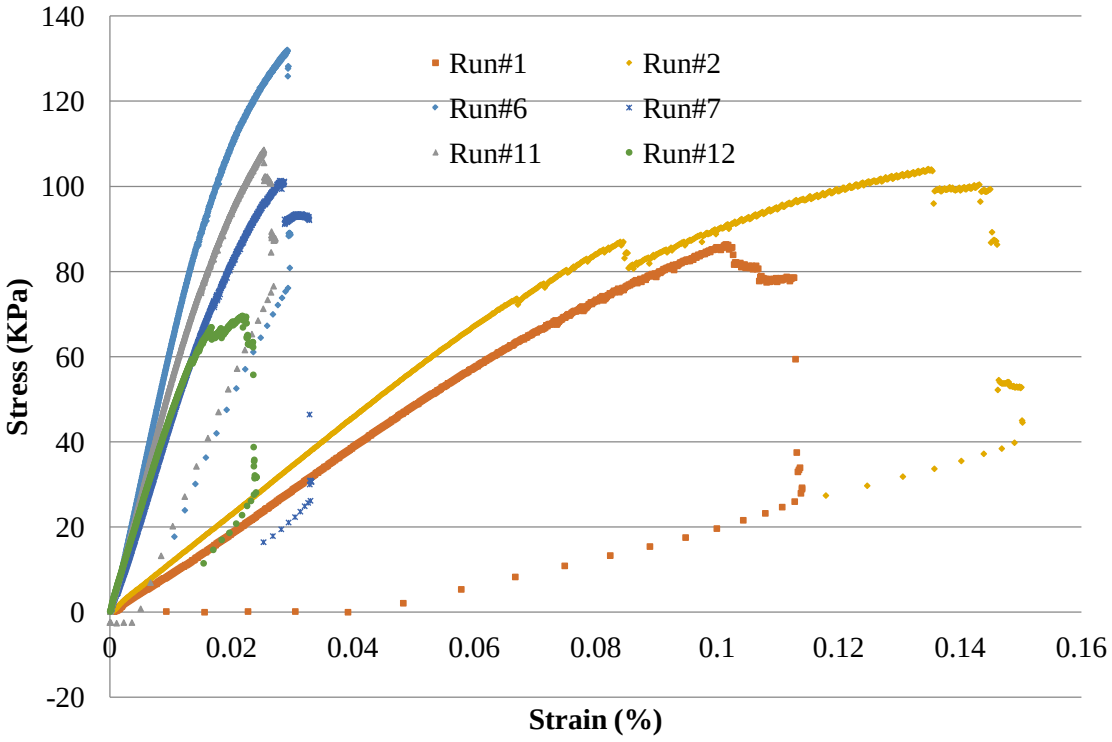

Figure 3.23 Stress strain curve of bending test for composite panels: resin A (Run #1, #2), B (Run #6, #7) and C (Run #11, #12).

3.4.3.3 Tension Parallel to Preferred Strand Orientation (machine direction)

Tension parallel to preferred strand orientation data was summarized and compared with published results in Table 3.10. The wood strand/epoxy vinyl ester composite tensile strength (77.13 MPa (COV = 20%)) was comparable to that of 20 vol% glass fiber/polyester composite with RTM processing (85 MPa). Its

tensile modulus are approximately 10 times the tensile modulus of extruded wood/pp composites, sisal/vinyl, hemp/polyester and glass fibers/polyester composites made with RTM.

Statistical analysis indicates that resin type significantly influenced the tensile strength (p-value<0.05) but not the tensile modulus (p-value>0.05) in Table 3.13. Fisher's LSD test for resin pairs (Table 3.14) was therefore established for tensile strength, which indicated that that resin A was statistically different form the other two resins, which can be attributed to the higher tensile strength for resins B and C compeering to resin A (83 MPa vs. 59 MPa) (Table 3.1) and better bonding achieved between strands and matrix with higher viscosity resins. Influence of resin types on flexural properties were shown in Figure 3.24 and Figure 3.25.

Table 3.13 ANOVA table of tensile strength and tensile modulus.

	Source	Df	SumSq	MeanSq	F value	Pr(>F)
Tensile strength	Resin	2	2379	1189.7	6.022	0.0171*
	Residuals	1	2173	197.6		
Tensile modulus	Resin	2	4.621	2.311	1.682	0.231
	Residuals	1	15.112	1.374		

*significant variable or interaction

Table 3.14 Fisher's LSD test of resin pairs of tensile strength.

Resin	Mean	Group[1]
A	47.57	a
B	75.67	b
C	77.13	b

[1] Means with the same letter are not significantly different.

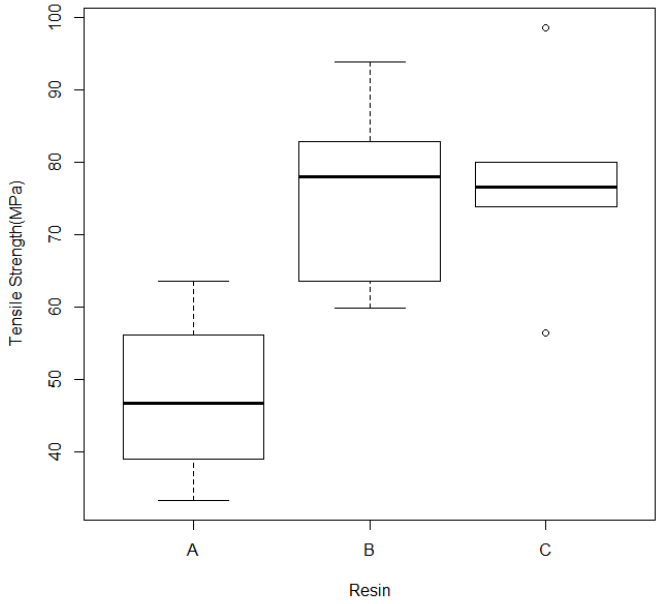

Figure 3.24 Influence of resin type on RTM wood strands panels with AL mold of tensile strength.

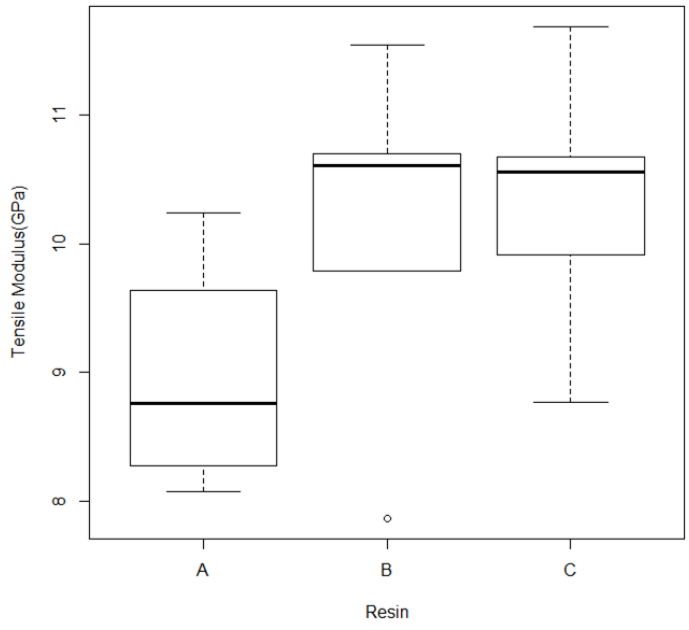

Figure 3.25 Influence of resin type on RTM wood strands panels with AL mold of tensile modulus.

3.4.3.4 Internal Bond (Tension Perpendicular to Surface)

Internal bond (IB) data was summarized and compared with published results in Table 3.10. IB strength for the molded composite panel is over two times (1.69-1.80 vs. 0.57-0.71 MPa) that of OSB made with hybrid poplar. Failure generally occurred near the core of the specimen and by wood failing (at the interfacial layer between wood strands and resin) (Figure 3.26). Note that the IB strength for quaking aspen (12% moisture content), which is in the same family as hybrid poplar, is 1.79 MPa. Similarities in these results along with the fact that typically failure was in the wood instead of on wood resin bonding, indicates that all three resins effectively bonded the strands.

Figure 3.26 Failure surfaces after IB tests.

Statistical analysis showed that IB strength was not significantly influenced by the resin type (p-value = 0.877). Resin A exhibited the highest deviation in IB strength and resin C the lowest variation (Figure 3.27).

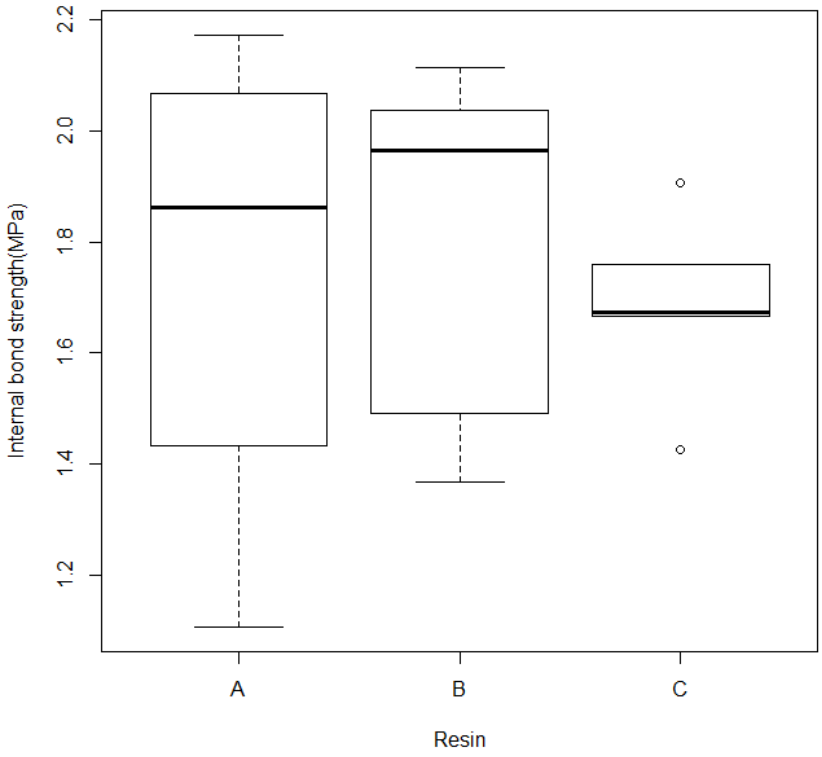

Figure 3.27 Internal bond strength and its relation to resins.

3.4.3.5 Water Absorption and Thickness Swell

Water absorption and thickness swell results are summarized in Table 3.15. Starved (dry) surfaces within a RTM panel will exhibit very poor dimensional stability properties (Figure 3.28). The comparison of average WA and TS for resins A, B and C are shown in Figure 3.29. Resin A shows the worst water resistance property and resin C shows the best among the three resin types. Resins filled the voids between the wood strands and created a barrier effect, thus preventing moisture from penetrating into the interstitial space. Moisture diffusion into cell wall seems to have been reduced significantly as evident

from the reduced thickness swell values. Shrinkage and swelling of wood is dominated by the shrinkage and swelling of cell wall (Siau, 1995). Although resins B and C (higher viscosity resins) yielded lower WA and TS, statistical analysis reveals no difference among the three resins (Table 3.16 to Table 3.18).

a) Specimen #4 shows poor dimensional stability

b) Specimen #15 shows good dimensional stability

Figure 3.28 Specimen condition after 24-h of submersion in water.

Table 3.15 Water absorption and thickness swell results

Resin System[a]	Specimen Number	WA[b]				TS[c]		Moisture content
		2h	24h	2h	24h	2h	24h	
		By Weight (%)		By Volume (%)[d]		%		%
A	1	5.20%	12.36%	5.71%	15.80%	5.43%	14.70%	5.20
	2	5.97%	15.31%	6.42%	10.13%	6.23%	9.00%	5.97
	3	5.37%	12.56%	1.66%	3.36%	1.46%	2.43%	5.37
	4	29.52%	34.32%	19.09%	30.13%	17.13%	27.41%	29.52
	5	2.04%	4.30%	0.29%	3.01%	0.32%	2.90%	2.04
	AVE[e]	4.64%	11.13%	3.52%	8.08%	3.36%	7.26%	4.64
	COV %	0.38	0.43	0.85	0.76	0.87	0.80	0.38
B	6	2.94%	6.12%	1.28%	1.48%	1.26%	1.06%	2.94
	7	3.90%	8.05%	4.94%	10.70%	4.87%	10.14%	3.90
	8	3.65%	7.27%	1.19%	5.01%	1.16%	4.53%	3.65
	9	4.16%	7.81%	0.68%	2.94%	0.65%	2.62%	4.16
	10	4.28%	7.60%	0.91%	2.44%	0.89%	2.18%	4.28
	AVE	3.79%	7.37%	1.80%	4.51%	1.77%	4.11%	3.79
	COV %	0.14	0.10	0.98	0.82	0.99	0.88	14.02
C	11	4.22%	7.39%	0.20%	5.11%	0.19%	4.91%	4.22
	12	5.36%	9.50%	3.84%	5.83%	3.77%	5.42%	5.36
	13	2.53%	4.99%	0.65%	2.25%	0.59%	1.96%	2.53
	14	3.18%	5.96%	3.44%	10.93%	3.32%	10.45%	3.18
	15	2.67%	5.28%	1.84%	6.17%	1.80%	5.99%	2.67
	AVE	3.59%	6.63%	1.99%	6.06%	1.93%	5.75%	3.59
	COV %	0.33	0.28	0.81	0.52	0.82	0.53	33.12

[a] resin system A, B and C represent unsaturated polyester, vinyl ester and epoxy vinyl ester, respectively.
[b] WA, water absorption
[c] TS, thickness swell
[d] The density of water is considered as 1 kg m^{-3}
[e] Specimen #4 is excluded from the average and coefficient of variation data

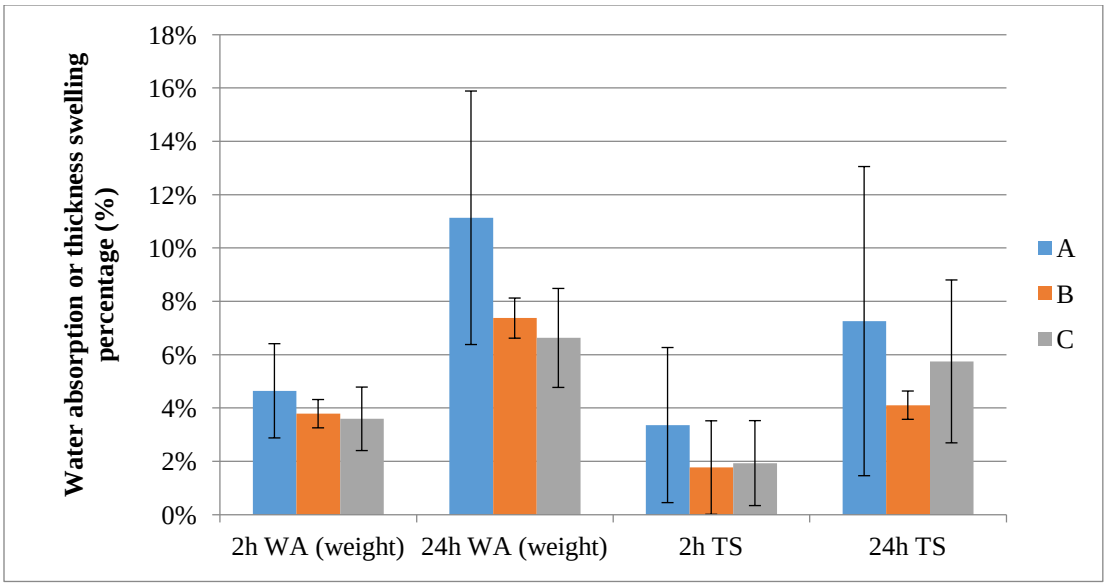

Figure 3.29 Comparison of WA and TS for resin system A, B and C.

Table 3.16 ANOVA table for 24-h water absorption measured by weight.

Source	Df	SumSq	MeanSq	F-value	Pr(>F)
Resin	2	0.0050	0.0025	3.2940	0.0757
Residuals	11	0.0084	0.0008		

Table 3.17 ANOVA table for 24-h water absorption measured by volume.

Source	Df	SumSq	MeanSq	F-value	Pr(>F)
Resin	2	0.0028	0.0014	0.7560	0.4930
Residuals	11	0.0205	0.0019		

Table 3.18 ANOVA table for 24-h thickness swell.

Source	Df	SumSq	MeanSq	F-value	Pr(>F)
Resin	2	0.0022	0.0011	0.6450	0.5430
Residuals	11	0.0190	0.0017		

3.4.4 Young's Modulus Estimation

Tensile strength and tensile modulus of tested wood strands are summarized in

Table 3.19.

Table 3.19 Tensile properties and grain angle of wood strands.

Strand number	Tensile strength (MPa)	Tensile modulus (GPa)
1	17.419	0.474
2	16.811	0.440
3	27.359	0.572
4	22.702	0.352
5	26.465	0.474
6	19.692	0.499
7	28.559	0.484
8	37.431	0.501
9	14.447	0.355
10	23.883	0.483
11	16.312	0.465
12	19.167	0.410
13	15.714	0.549
14	23.127	0.509
15	16.643	0.485
16	26.739	0.525
Average	22 (28.14%)[1]	0.480 (29.79%)

[1] Data in parenthesis is coefficient of variation in percentage.

Estimated volume fractions and composite's predicted Young's modulus in tension are presented in Table 3.21. The predicted lower Young's modulus (2.37 GPa) is much lower than experimentally determined Young's modulus (10.32 GPa) (Tables 3.20 and 3.21). Measured wood strand density is 508 kg m^{-3}. Findings indicate that Young's modulus of wood strands is probably modified due to partial densification and resin infusion (that aids in repairing strand damage that occurs in the flaking or stranding process) during the RTM process. It is widely known that the mechanical properties of wood are highly correlated

with specific gravity. The relationship between density and a property (such as modulus) is expressed in Equation 3.21 (Bodig & Jayne, 1982).

$$Y = aD^b \qquad \text{Equation 3.21}$$

where, a, b are parameters determined by the particular mechanical property, and D is the specific gravity. Constants in Equation 3.21 can be obtained by least square fit to experimental data for a wide range of species (Table 3.20 presents values of constants as suggested by Bodig and Jayne (1982)).

Table 3.20 Constants for the relationship between mechanical properties and SG for wood (Bodig & Jayne, 1982).

Mechanical property	a	b
E (GPa)	19.3	1.00

Based on this approximate relationship between Young's modulus and density, wood strand modulus can be adjusted to account for an increase in its value due to strand densification during the RTM process to predict the composite modulus. However, as it is difficult to accurately predict the extent of strand densification. Another approach is to determine the upper and lower boundaries of E_x by determining corresponding stand modulus at lower and upper density limits. Lower boundary for strand specific gravity is assumed in this study to be equal to the hybrid poplar wood specific gravity (0.36); whereas, the upper limit is assumed to be the specific gravity when the void volume is close to zero. Strand density with no voids, essentially the cell wall specific gravity, is assumed to be 1.5 on the average (Bodig & Jayne, 1982).

Based on assumed lower and upper limits of strand density and applying Equations 3.21 and 3.17, lower and upper limits of wood strand composite panel's Young's modulus were calculated (Table 3.21). Experimentally determined Young's modulus falls between the upper and lower boundaries calculated. This can be attributed to the densification of the wood strands during preform fabrication and the RTM process, as well as resin infusion that repairs strands. Based on the composite Young's modulus

determined experimentally, strand specific gravity during the RTM process was estimated to have increased to 1.05, which is known to happen in a hot pressing process of strand composites under heat and pressure. Further investigation of changes to strand density and properties need to be evaluated to confirm that rule of mixtures is effective in predicting composite elastic properties.

Table 3.21 Predicted Young's modulus and related component values used in prediction.

Average wood strand density (kg m^{-3})	508 (15.31%)[a]
Average resin Young's modulus (GPa)	3.63 (10.45%)
Average fiber volume fraction	0.3994 (10.80%)
Predicted panel Young's modulus (GPa)	2.3719
Observed panel Young's modulus (GPa)	10.32 (9.49%)
Lower boundary of panel Young's modulus (GPa)	6.95
Upper boundary of panel Young's modulus (GPa)	28.98
Young's modulus with wood D=1.05 (GPa)	10.27

[a] Data in parentheses is coefficient of variation in percentage.

3.5 Conclusions and Recommendations

The primary objective in this part of the overall study was to evaluate the influence of RTM processing parameters on a composite panel performance and develop benchmark performance values for wood strand composite panels produced using the RTM process. In this study, preform parameters and processing variables that significantly influence the composite plane performance have been identified using a response surface analysis and D-optimal design. Based on these results, robust statistical analysis, such as factorial analysis, can be performed to establish structure-process-property relationships.

Similar to what has been found in the case of synthetic fiber panels, preform permeability is directly related to preform density (proportional to fiber volume fraction), and similar to studies conducted on other fiber preforms. Injection pressure showed a positive influence on permeability. Specific permeability determined using the three methods implemented in this study yielded similar values, except higher permeability with higher preform porosity was computed using the third method. Method one,

which was directly generated from Darcy's law and two, which was based on the averaged flow velocity are recommended for less homogeneous preforms.

Vacuum is a key factor in determining the surface quality of an RTM produced composite. High vacuum (~85 KPa) leads to a good surface finish, as it is believed to expel air in preform. MOR and MOE performance is highly dependent on fiber preform density, which agrees with the published data. Higher density fiber preform can transfer stress from fiber to matrix and also reduce stress concentration. Injection pressure at 138 to 207 KPa, and vacuum at 85 KPa were applied in manufacturing specimens for benchmark value determination.

All panels produced using RTM had a homogeneous density distribution across the panel thickness, yielding good panel quality with little variation. Mechanical and physical properties of RTM wood strand panels were superior to many currently produced wood strand panels (MOR = 98.74 MPa (COV=18.35%); MOE = 10.32 GPa (9.48%); tensile strength = 68.16 MPa (27.46%); tensile modulus = 9.85 GPa (12.49%); and internal bond strength = 1.74 MPa (17.86%)). Resin viscosity coupled with resin strength tends to yield higher performance panels. All three resin types resulted in excellent bonding between strands as indicated by the internal bond test values.

Of most significance is that RTM produced panels yielded significantly lower water absorption and thickness swell values. Therefore, it can be concluded that RTM technology can be utilized to produce wood strand panels of better mechanical performance (compared with OSB and similar composite products) with good dimensional stability when exposed to moisture rich environments.

All the three resin used in this study have high styrene content, which is considered as hazardous material and proper care is required when processing with them. Therefore, styrene free resin should be considered for researchers. CCP composites launched Encore Prime styrene free resin both for unsaturated polyester and vinyl ester resins with even higher tensile and flexural properties (CCP composites, n.d.). Additionally, additives can be applied to the resins to improve ductility of the resulting panels if needed.

3.6 References

Amico, S., & Lekakou, C. (2001). An experimental study of the permeability and capillary pressure in resin-transfer moulding. Composites Science and Technology, 61(13), 1945–1959. doi:10.1016/S0266-3538(01)00104-X

Arbter, R., Beraud, J. M., Binetruy, C., Bizet, L., Bréard, J., Comas-Cardona, S., … Ziegmann, G. (2011). Experimental determination of the permeability of textiles: A benchmark exercise. Composites Part A: Applied Science and Manufacturing, 42(9), 1157–1168. doi:10.1016/j.compositesa.2011.04.021

Barraza, H. J., Hamidib, Y. K., Aktasb,, L., O'Rear, E. a., & Altan, M. C. (2004). Porosity Reduction in the High-Speed Processing of Glass-Fiber Composites by Resin Transfer Molding (RTM). Journal of Composite Materials, 38(3), 195–226. doi:10.1177/0021998304038649

Bickerton, S., & Abdullah, M. Z. (2003). Modeling and evaluation of the filling stage of injection/compression moulding. Composites Science and Technology, 63(10), 1359–1375. doi:10.1016/S0266-3538(03)00022-8

Bodig, J., & Jayne, B. A. (1982). Mechanics of wood and wood composites. New York: Van Nostrand Reinhold.

Buntain, M. J., & Bickerton, S. (2003). Compression flow permeability measurement: a continuous technique. Composites Part A: Applied Science and Manufacturing, 34(5), 445–457. doi:10.1016/S1359-835X(03)00090-3

Caba, K. D. la, Guerrero, P., Eceiza, A., & Mondragon, I. (1996). Kinetic and rheological studies of an unsaturated polyester cured with different catalyst amounts. Polymer, 37(2), 275–280.

CCP composites. (n.d.). Encore ® prime styrene free product range, pp. 1–2.

Daniel, I. M. (2007). Observation of Permeability Dependence on Flow Rate and Implications for Liquid Composite Molding. Journal of Composite Materials, 41(7), 837–849. doi:10.1177/0021998306067061

Demaria, C., Ruiz, E., & Trochu, F. (2007). In-plane anisotropic permeability characterization of deformed woven fabrics by unidirectional injection. Part I: Experimental results. Polymer Composites. doi:10.1002/pc

Ferland, P., & Trochu, F. (1996). Resin Transfer Molding, 17(1).

Francucci, G., & Vázquez, A. (2012). Capillary effects in vacuum-assisted resin transfer molding with natural fibers. Polymer …. doi:10.1002/pc

Haider, M., Hubert, P., & Lessard, L. (2007). An experimental investigation of class A surface finish of composites made by the resin transfer molding process. Composites Science and Technology, 67(15-16), 3176–3186. doi:10.1016/j.compscitech.2007.04.010

Hayward, J., & Harris, B. (1990). The effect of vacuum assistance in resin transfer moulding. Composites Manufacturing.

Hossain, M., Islam, M., Vuurea, A., & Verpoest, I. (2013). Effect of Fiber Orientation on the Tensile Properties of Jute Epoxy Laminated Composite. Journal of Scientific Research.

Idicula, M., Sreekumar, P. A., Joseph, K., & Thomas, S. (2009). Natural Fiber Hybrid Composites — A Comparison Between Compression Molding and Resin Transfer Molding. Polymer Composites. doi:10.1002/pc

Khan, R. a., Khan, M. a., Zaman, H. U., Parvin, F., Islam, T., Nigar, F., … Mustafa, a. I. (2011). Fabrication and Characterization of Jute Fabric-Reinforced PVC-based Composite. Journal of Thermoplastic Composite Materials, 25(1), 45–58. doi:10.1177/0892705711404726

Leclerc, J. S., & Ruiz, E. (2008). Porosity reduction using optimized flow velocity in Resin Transfer Molding. Composites Part A: Applied Science and Manufacturing, 39(12), 1859–1868. doi:10.1016/j.compositesa.2008.09.008

Lee, G.-W., Lee, N.-J., Jang, J., Lee, K.-J., & Nam, J.-D. (2002). Effects of surface modification on the resin-transfer moulding (RTM) of glass-fibre/unsaturated-polyester composites. Composites Science and Technology, 62(1), 9–16. doi:10.1016/S0266-3538(01)00091-4

Lekakou, C., & Bader, M. G. G. (1998). Mathematical modelling of macro- and micro-infiltration in resin transfer moulding (RTM). Composites Part A: Applied Science and Manufacturing, 29(1-2), 29–37. doi:10.1016/S1359-835X(97)00030-4

Li, Y. (2006). Processing of Sisal Fiber Reinforced Composites by Resin Transfer Molding. Materials and Manufacturing Processes, 21(2), 181–190. doi:10.1081/AMP-200068669

Lundström, T. S., Stenberg, R., Bergström, R., Partanen, H., & Birkeland, P. A. (2000). In-plane permeability measurements: a nordic round-robin study. Composites Part A: Applied Science and Manufacturing. doi:10.1016/S1359-835X(99)00058-5

Ma, Y., & Shishoo, R. (1999). Permeability Characterization of Different Architectural Fabrics. Journal of Composite Materials, 33(8), 729–750. doi:10.1177/002199839903300805

Naffakh, M., Dumon, M., & Gerard, J. (2006). Study of a reactive epoxy–amine resin enabling in situ dissolution of thermoplastic films during resin transfer moulding for toughening composites. Composites Science and Technology, 66(10), 1376–1384. doi:10.1016/j.compscitech.2005.09.007

Naik, N. K., Sirisha, M., & Inani, a. (2014). Permeability characterization of polymer matrix composites by RTM/VARTM. Progress in Aerospace Sciences, 65, 22–40. doi:10.1016/j.paerosci.2013.09.002

Pomeroy, R. (2009). Permeability characterisation of continuous filament mats for resin transfer moulding. Retrieved from http://pearl.plymouth.ac.uk/handle/10026.1/2691

Rodriguez, E., Giacomelli, F., & Vazquez, a. (2004). Permeability-Porosity Relationship in RTM for Different Fiberglass and Natural Reinforcements. Journal of Composite Materials, 38(3), 259–268. doi:10.1177/0021998304039269

Rouison, D., Sain, M., & Couturier, M. (2004). Resin transfer molding of natural fiber reinforced composites: cure simulation. Composites Science and Technology, 64(5), 629–644. doi:10.1016/j.compscitech.2003.06.001

Siau, J. F. (1995). Wood--influence of moisture on physical properties. (V. P. I. and S. U. D. of W. S. & F. Products, Ed.). Blacksburg, VA]: Blacksburg, VA : Dept. of Wood Science and Forest Products, Virginia Polytechnic Institute and State University.

Umer, R., Bickerton, S., & Fernyhough, a. (2007). Characterising wood fibre mats as reinforcements for liquid composite moulding processes. Composites Part A: Applied Science and Manufacturing, 38(2), 434–448. doi:10.1016/j.compositesa.2006.03.003

Yadama, V., & Wolcott, M. (2006). Elastic properties of hot-pressed aspen strands. Wood and Fiber Science. Retrieved from http://swst.metapress.com/index/58K5337703K454QX.pdf

Chapter 4 Conclusions and Recommendations

The goal of this research was to investigate and develop the underpinnings of resin transfer molding (RTM) wood strand composite panels with superior mechanical and physical properties. This research focused on determining suitable wood strands preform fabrication parameters and processing variables during resin transfer. Moreover, resin flow behavior was characterized with three different resins and benchmark performance values for RTM composite panels were evaluated.

Three processing variables (target density, PVAc content and pre-pressing duration) and three responses (handling, void volume and actual density) were investigated. Preform handling improved with increased target density and PVAc content. Duration of pre-pressing was not a significant factor, thus was fixed at 600 seconds for further analysis and RTM of composite panels to evaluate their properties.

Permeability was determined using three different methods. Preform permeability was directly proportional to injection pressure. Flexural performance (MOR, MOE) of composite panels increased with increasing injection pressure and vacuum. Surface property was highly influenced by vacuum level; higher vacuum corresponded to better surface finish.

Results from the vertical density profile indicated a homogeneous density through the panel thickness. Resin viscosity and type definitely influences the composite panel performance. All three resins (unsaturated polyester, vinyl ester and epoxy vinyl ester), however, produced RTM panels with superior performance than many existing commercially produced wood strand composite panels. High internal bond strength indicated excellent bonding between wood strands. In addition to superior mechanical properties, RTM panels had far greater resistance to moisture than wood strand composites such as OSB. Results of dimensional stability indicate a potential for using these panels in moisture-rich environment.

The next phase of the overall study will focus on further understanding the effects of processing variables including fiber orientation. A comprehensive factorial analysis can be devised based on the screening

analysis done in this study to establish structure-process-property relationships. Then, the next step in technology will involve producing profile composite products using VARTM with vacuum bagging for wood strand preforms. Influence of processing factors including resin viscosity, injection pressure, and vacuum will be determined for VARTM with vacuum bags. Additionally, finite element method (FEM) can be applied to simulate the resin flow and evaluate factors affecting preform permeability. Moreover, injection port and vent location can also be easily designed and simulated in VARTM with FEM to achieve composite panels with better performance, both cosmetic and mechanical.

Further research is also needed on use of resins with lower environmental impact, such as resins with less styrene emission. Resin curing in the mold at higher temperatures needs to be explored as well to shorten curing time for efficient processing and achieving cost-effectiveness.

APPENDICES

Appendix A RTM Pneumatic Injection System Overview

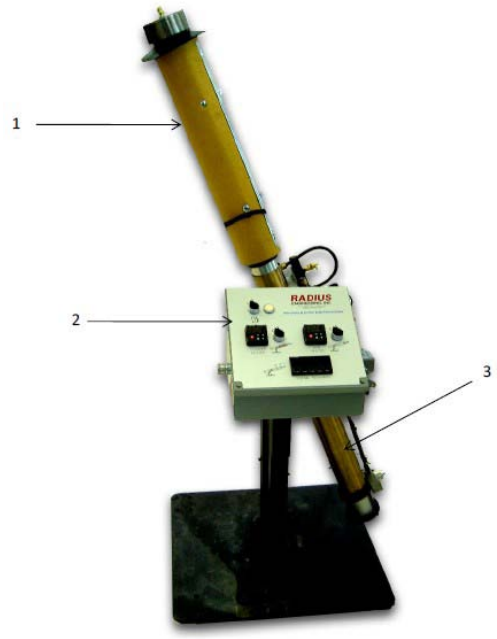

Figure A.1 Pneumatic injection cylinder: 1) Injection Cylinder, 2) Controls Interface Panel and 3) Pneumatic Cylinder (Radius Engineering, n.d.).

Appendix B DSC Testing

Differential scanning calorimetry (DSC) wad used to determine the proper catalyst content. The boiling temperature for styrene is 145 °C, according to some investigators (Beheshty, Nasiri, & Vafayan, 2005), when the heating rate is over 30 °C/min, the pressure inside the closed DSC pan is approximately 2 bar, which causes evaporation of styrene. Thus, the resin can occur simultaneously to curing. And for the heating rate lower than 5 °C/min, some of the initial and final reaction cannot be recorded due to the lack of sensitivity. Dynamic scan was performed at six levels: 5, 10, 15, 20, 25 and 30°C/min with the temperature ranges from 20°C to 200°C. The DSC runs have made up to 200°C to avoid thermal decomposition, which has been proved by thermogravimetric analysis (TGA), as illustrated in Figure B.1. The decomposition begins around 200°C, and the sample has almost finishes its decomposition procedure at about 450°C. Several methods were applied to study the cure property.

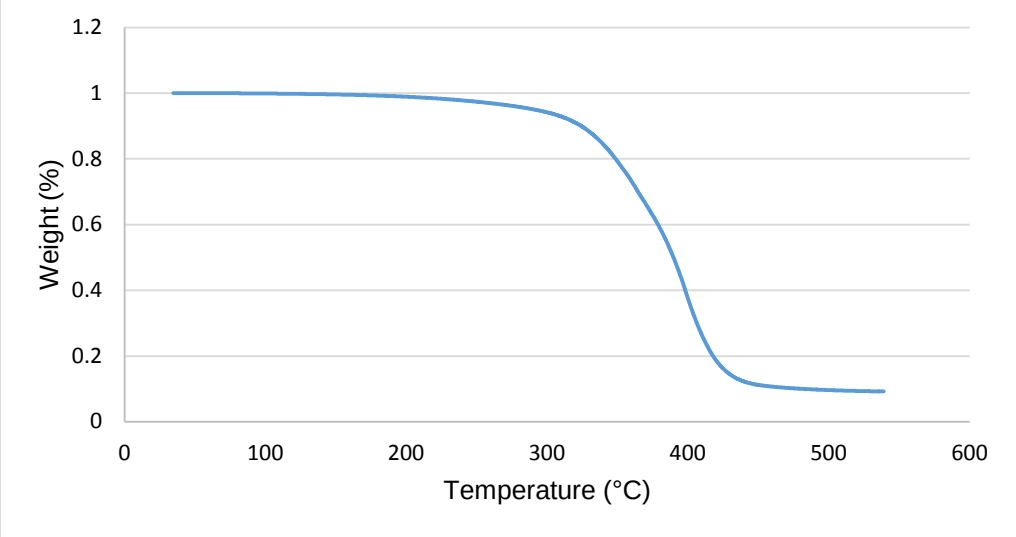

Figure B.1 TGA graph for cured UPE with 1% MEKP content.

Kissinger's Method

Kissinger's corrected kinetic equation is the most typical and extensive model that is prevailingly applied to evaluate the kinetic reactions (Hsieh, 2010). By obtaining the slope of $ln(\frac{\beta}{T_p^2})$ and $1/T_p$ in Equation B.1, the E_K of the sample can be determined (B.V.Erofeev (Institute of Physical Organic Chemistry), 1965; Hsieh, 2010).

$$ln\left(\frac{\beta}{T_p^2}\right) = ln\frac{AR}{E_K} - \frac{E_K}{RT_P} \qquad \text{Equation B.1}$$

where β is heating rate ($°C/min$), A is the pre-exponential factor ($1/sec$), E_K is the activation energy (KJ/mol), the subscript K represents Kissinger's method, T_p is the peak temperature (K), R is the gas constant($= 8.314\ J/mol\ k$).

Ozawa's Method

Another very commonly used method is the Ozawa equation (Heireche & Belhadji, 2007; Mušanić, 2010; Ozawa, 1965) which can be derived from the basic kinetic equation for the special case of dynamic DSC with constant heating rate: $\beta = dT/dt$. When a series of experiments are conducted at different heating rates, the linear regression of $log(\beta)$ to the reciprocal absolute peak temperature $1/T_p$ generates the activation energy, expressed in the following Equation B.2:

$$log(\beta) \cong -0.4567\frac{E_o}{R} \cdot \frac{1}{T_p} \qquad \text{Equation B.2}$$

where β is heating rate (°C/min), E_O is the activation energy (KJ/mol), the subscript o represents Ozawa method.

Crane Equation

Crane equation is expressed in Equation B.3, when $\frac{E}{nR}$ is larger than $2T_p$, plot of $ln\,\beta$ verses the reciprocal absolute peak temperature, the slope of the linear regression of the curve is $-\frac{E}{nR}$ with the activation energy obtained by Kissinger method, the degree of reaction was determined.

$$\frac{d(ln\beta)}{d(\frac{1}{T_p})} = -(\frac{E_{a,k}}{nR} + 2T_p) \qquad \text{Equation B.3}$$

Curing Behaviors

Figure B.2 shows that with the increases of the catalyst content from 1.0% to 2.5%, the peak exothermic reaction time decrease from 11-minute to 3-minute. Higher MEKP content corresponds to fast curing. Therefore, 1.0% MEKP content was chosen. Figure B.3 present the DSC thermograms of curing of polyester and vinyl ester at different heating rate. As the heating rate increased, the peak exothermic temperatures shifted to higher temperatures. Figure B.4 and Figure B.5 depict the linear regression of the three methods. DSC results were summarized in Table B.1, as can be seen that the activation energy for polyester is lower than that of vinyl ester, which implying polyester reacts easily during curing. However, vinyl ester has higher degree of reaction. Post curing is necessary to achieve complete cure.

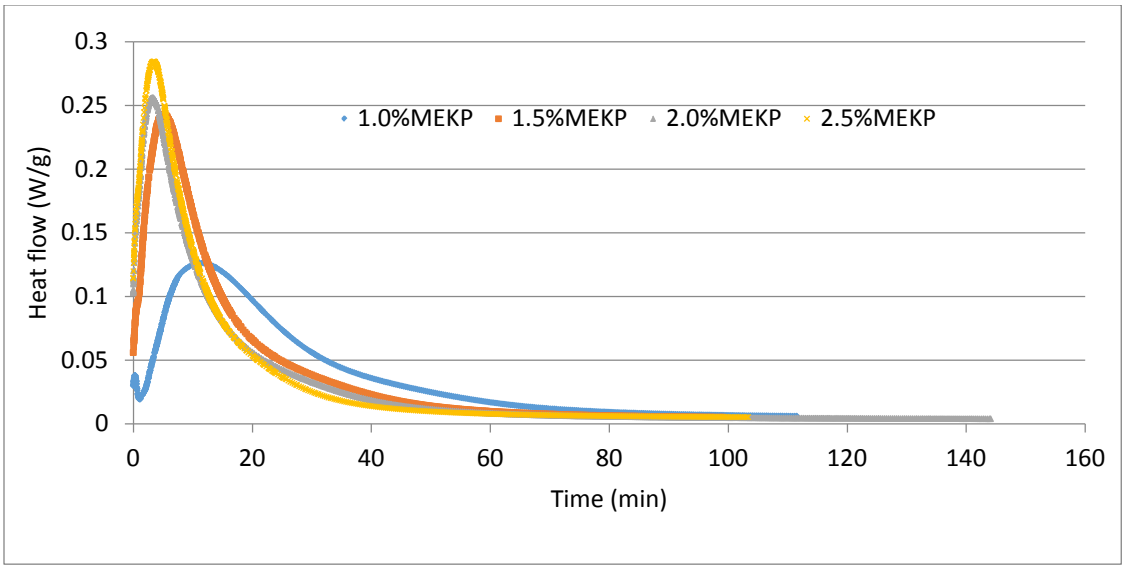

Figure B.2 DSC heat flow at 50°C isothermal

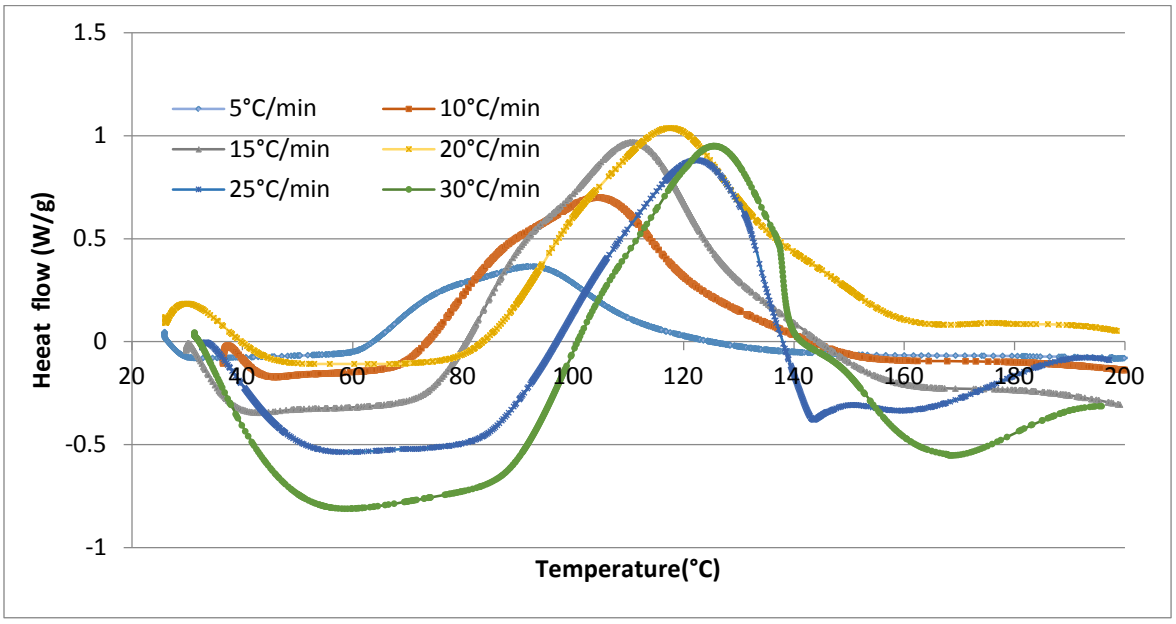

a) Polyester

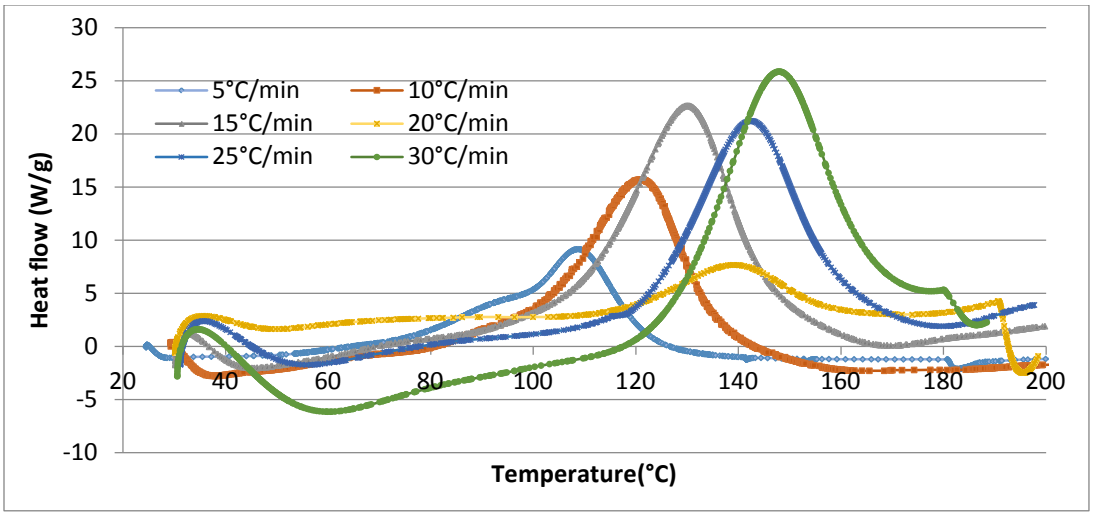

b) Vinyl ester

Figure B.3 DSC thermograms at different heating rates

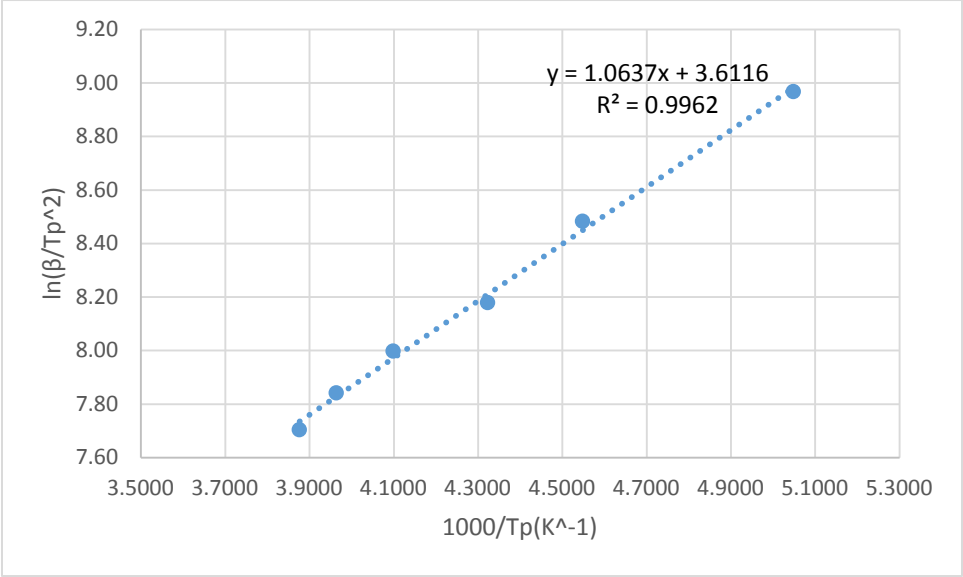

a) Kinssinger's method

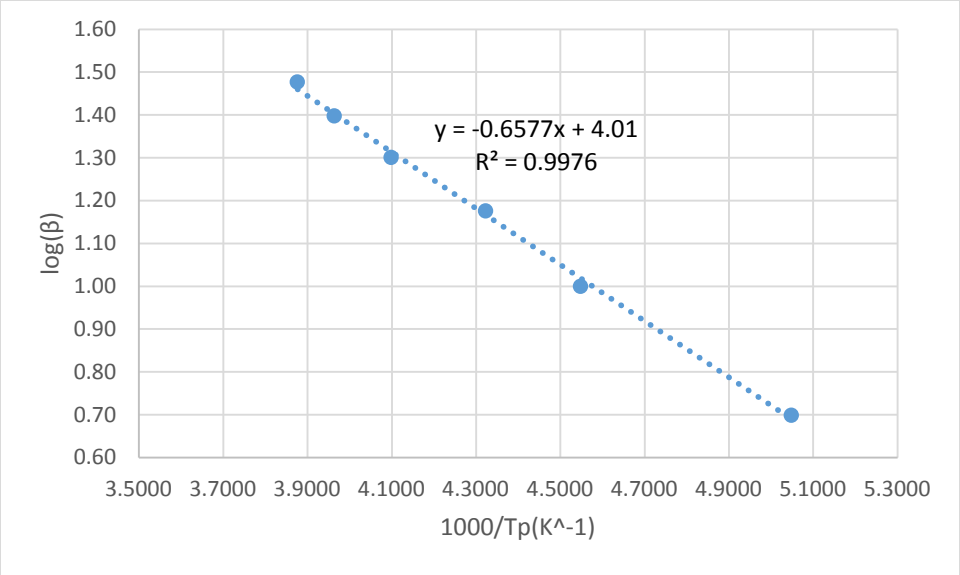

b) Ozawa's method

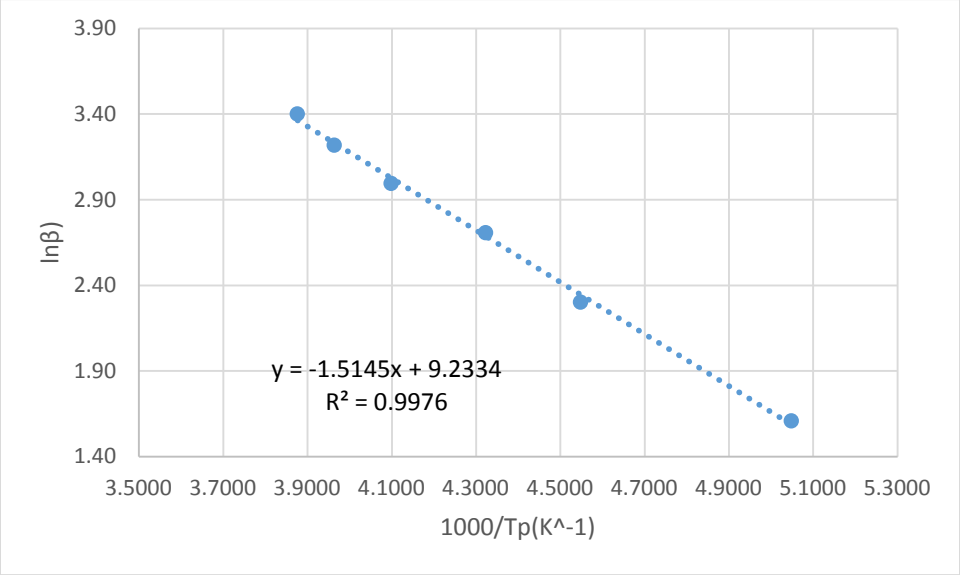

c) Crane's method

Figure B.4 Linear regression for polyester

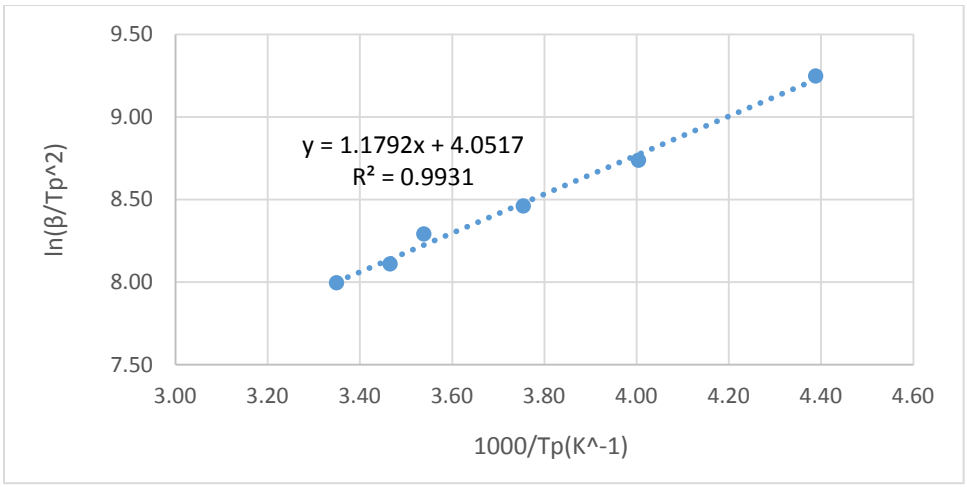

a) Kissinger's method

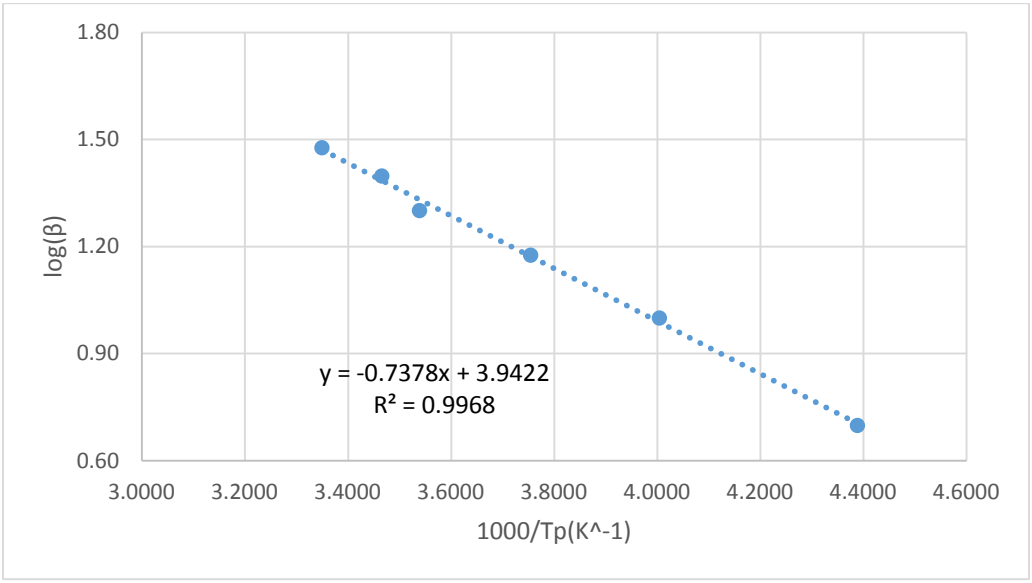

b) Ozawa's method

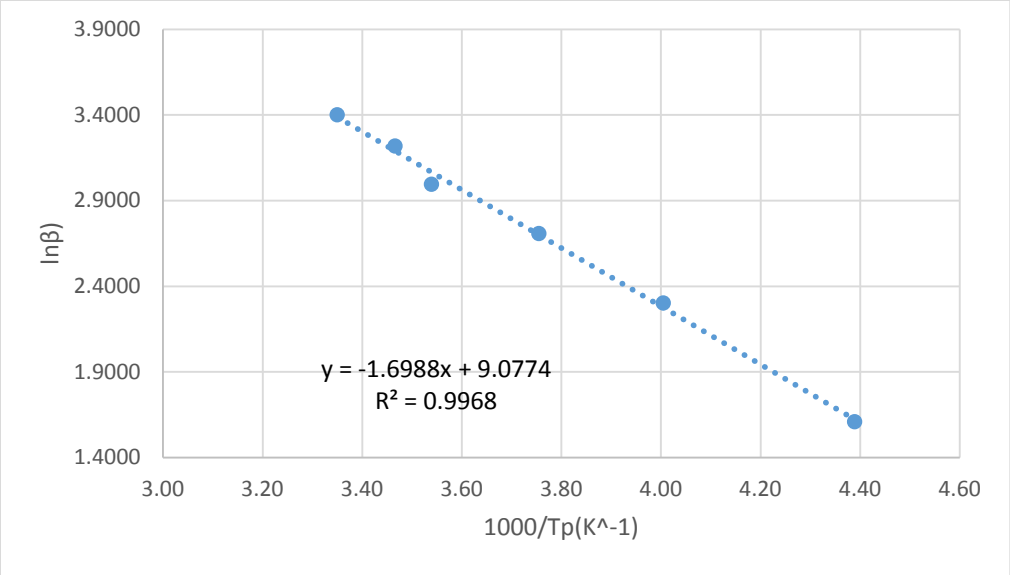

c) Crane's method

Figure B.5 Linear regression for vinyl ester

Table B.1 DSC results of polyester and vinyl ester.

Resin system	E_K (KJ mol^{-1})	E_O (KJ mol^{-1})	A	Degree of reaction
Polyester	8.84	11.973	39.38	70.20%
Vinyl ester	9.80	13.43	67.8	77.86%

Appendix C ANOVA table for permeability (K_2) and permeability (K_3)

Analysis of variance was also conducted with permeability estimation method two and three. The results were shown in Table C.1 and Table C.2. Similar to the first approach, resin viscosity and preform density were significant variables for permeability.

Table C.1 ANOVA for permeability approach one (K_2) with estimated coefficients.

Source	Sum of Squares	df	F-value	P-value	Coefficient
Model	24.2209	4	8.3558	0.0004*	3.0710
A-Injection pressure	2.8272	1	3.9013	0.0622	
B-vacuum	0.4985	1	0.6879	0.4167	
C-resin viscosity	10.3185	1	14.2388	0.0012*	0.0050
D-preform density	8.5506	1	11.7992	0.0026*	-0.0038
Residual	14.4935	20			
Lack of Fit	12.0045	17	0.8511	0.6515	
Pure Error	2.4890	3			

*Significant variables

Table C.2 ANOVA for permeability approach one (K_3) with estimated coefficients.

Source	Sum of Squares	df	F-value	P-value	Coefficient
Model	270.2979	4	10.5198	< 0.0001*	8.5000
A-Injection pressure	25.5525	1	3.9780	0.0599	
B-vacuum	1.3788	1	0.2146	0.6482	
C-resin viscosity	85.1647	1	13.2583	0.0016*	0.0142
D-preform density	95.2558	1	14.8292	0.0010*	-0.0159
Residual	128.4704	20	10.5198	< 0.0001	
Lack of Fit	111.8457	17	1.2310	0.4955	
Pure Error	16.6247	3			

*Significant variables

Reference

B.V.Erofeev (Institute of Physical Organic Chemistry). (1965). Reaction rates of processes involving solids with different specific surfaces. International Sumposium on Thermal Analysis, 273–282.

Beheshty, M., Nasiri, H., & Vafayan, M. (2005). Gel Time and Exotherm Behaviour Studies of an Unsaturated Polyester Resin Initiated and Promoted with Dual Systems. Iranian Polymer Journal, 14(11), 990–999.

Heireche, L., & Belhadji, M. (2007). The methods Matusita, Kissinger and Ozawa in the study of the crystallization of glasses. The case of Ge-Sb-Te alloys. Chalcogenide Letters, 4(2), 23–33.

Hsieh, Y.-C. (2010). Thermal Analysis of Multi-walled Carbon Nanotubes by Kissinger's Corrected Kinetic Equation. Aerosol and Air Quality Research, 212–218. doi:10.4209/aaqr.2009.08.0053

Koehler, A. (1955). Guide to determining slope of grain in lumber and veneer.

Mušanić, S. M. (2010). Applicability of non-isothermal DSC and Ozawa method for studying kinetics of double base propellant decomposition. … European Journal of …, 7(3), 233–251.

Ozawa, T. (1965). A New Method of Analyzing Thermogravimetric Data. Bulletin of the Chemical Society of Japan, 38(11), 1881–1886.

Radius Engineering, I. (n.d.). 2100cc Pneumatic RTM Injection System Operation & Maintenance Manual, 1(801), 1–39.